SINGLE-CELL MULTI-OMICS CHARACTERISE DISCRETE HUMAN TENDON CELLS POPULATIONS THAT PERSIST *IN VITRO* AND ON FIBROUS SCAFFOLDS

A. Gomez-Collignon[1], R. Brown[2], A. Carr[1], S. Dakin[1], A. Lach[1], C. Loizou[2], M. Rogers[2], R. Sharp[2] and A. Kendal[1,2,*]

[1] Botnar Research Centre, The Nuffield Department of Orthopaedics, Rheumatology and Musculoskeletal Sciences, Windmill Road, Oxford, OX3 7LD, UK
[2] Nuffield Orthopaedic Centre, Windmill Road, Oxford, OX3 7LD, UK

Abstract

Chronic tendinopathy represents a growing healthcare burden in the ageing global population. Curative therapies remain elusive as the mechanisms that underlie chronic inflammation in tendon disease remain unclear. Identifying and isolating key pathogenic and reparative cells is essential in developing precision therapies and implantable materials for improved tendon healing.

Multiple discrete human tendon cell populations have been previously described *ex vivo*. To determine if these populations persist *in vitro*, healthy human hamstring tenocytes were cultured for 8 d on either tissue culture plastic or aligned electrospun fibres of absorbable polydioxanone. Novel single-cell surface proteomics combined with unbiased single-cell transcriptomics (CITE-Seq) was used to identify discrete tenocyte populations.

6 cell populations were found, 4 of which shared key gene expression determinants with *ex vivo* human cell clusters: PTX3_PAPPA, POSTN_SCX, DCN_LUM and ITGA7_NES. Surface proteomics found that PTX3_PAPPA cells were CD10+CD26+CD54+. ITGA7_NES cells were CD146+ and POSTN_SCX cells were CD90+CD95+CD10+.

Culture on the aligned electrospun fibres favoured 3 cell subtypes (DCN_LUM, POSTN_SCX and PTX3_PAPPA), promoting high expression of tendon-matrix-associated genes and upregulating gene sets enriched for TNF-α and IL-6/STAT3 signalling.

Discrete human tendon cell subpopulations persisted in *in vitro* culture and could be recognised by specific gene and surface-protein signatures. Aligned polydioxanone fibres promoted the survival of 3 clusters, including pro-inflammatory *PTX3*-expressing CD10+CD26+CD54+ cells found in chronic tendon disease. These results improved the understanding of preferred culture conditions for different tenocyte subpopulations and informed the development of *in vitro* models of tendon disease.

Keywords: Tenocyte, tendon fibroblast, human tendon, single-cell RNA sequencing, CITE-Seq, transcriptomic, tendinopathy, *in vitro*, culture, polydioxanone, scaffolds, fibres.

* **Address for correspondence**: Adrian Kendal, Botnar Research Centre, The Nuffield Department of Orthopaedics, Rheumatology and Musculoskeletal Sciences, Windmill Road, Oxford, OX3 7LD, UK.
Email: adriankendal@hotmail.com

List of Abbreviations

ACTA2	alpha smooth muscle actin
ADT	antibody derived tag
APOD	apolipoprotein D
BSA	bovine serum albumin
CD	cluster of differentiation
CHI3L	chitinase-3-like protein 1
CITE-Seq	cellular indexing of trancriptomes and epitopes by sequencing
CLDN11	claudin 11
COL1A1	collagen 1 type 1
COL1A2	collagen 1 type 1
COL3A1	collagen 3 type 1
COL6A3	collagen 6 type 3
COL8A1	collagen 8 type 1
CTGF	connective tissue growth factor
CXCL	C-X-C motif chemokine ligand
DCN	decorin
DKK1	Dickkopf-related protein 1

DMEM	Dulbecco's modified Eagle medium
ELN	elastin
FAP	fibroblast activation protein
FBLN	fibulin
FBN1	fibrillin 1
FCS	foetal calf serum
FGF	fibroblast growth factor
FMOD	fibromodulin
FN	fibronectin
HAS2	hyaluronan synthase-2
HFIP	1,1,1,3,3,3-hexafluoro-2-propanol
HTO	hashtag oligo antibody
IFN-γ	interferon-gamma
IL	interleukin
IL7R	interleukin 7 receptor
ITGA7	integrin subunit alpha 7
JAK	Janus kinase
KRT7	keratin 7
LUM	lumican
MKI67	marker of proliferation Ki-67
MMP	matrix metalloproteinase
Mtorc1	mammalian target of rapamycin complex 1
MYL9	myosin light chain 9
MYF5	myogenic factor 5
NAMPT	nicotinamide phosphoribosyltrasferase
NF-κB	nuclear factor kappa beta
NOTCH3	Notch receptor 3
PAPPA	pappalysin 1
PBS	phosphate-buffered saline
PC	principal components
PCA	principal component analysis
PCNA	proliferating cell nuclear antigen
PDGF	platelet-derived growth factor
PDO	polydioxanone
PDS	polydioxanone
PECAM1	platelet endothelial cell adhesion molecule 1
PENK	proenkephalin
POSTN	periostin
PRELP	proline and arginine rich end leucine rich repeat protein
PSM	polydioxanone suture material
PTX3	pentraxin 3
RGS5	regulator of G signaling protein
SCX	scleraxis
SEM	scanning electron microscope
SNN	shared nearest neighbor
SOD2	superoxide dismutase 2
STAT	signal transducer and activator of transcription
TAGLN	transgelin
TGFB1	transforming growth factor beta 1
THY1	cluster of differentiation 90
TNF-α	tumour necrosis factor alpha
TOP2A	DNA topoisomerase II alpha
TPPP	tubulin polymerisation promoting protein
TPSC	tendon progenitor stem cell
UMAP	uniform manifold approximation and projection
UMI	unique molecular identifier
VEGF	vascular endothelial growth factor
VWF	von Willebrand factor
WNT5A	Wnt family member 5a

Introduction

Musculoskeletal disorders are a major cause of long-term morbidity, being the second cause of most years lived with disability worldwide (Forouzanfar *et al.*, 2015). Chronic tendinopathy affects over 20 % of the population, with lower-limb tendinopathy being responsible for reduced mobility, tendon rupture, deformity and ultimately degeneration of small weight-bearing joints (Albers *et al.*, 2016; de Jonge *et al.*, 2011; Riel *et al.*, 2019). Chronic tendinopathy is characterised by painful and persistent inflammation, with a loss of regular structural organisation of the extracellular matrix. At the cellular level, tendinopathic tendons experience a surge in cellularity through an expansion of fibroblasts and endothelial cells. Fibroblasts respond to matrix damage during tendinopathy by depositing glycosaminoglycans and collagen type III in the extracellular matrix, leading to irregular collagen fibril alignment. Over time, the accumulation of collagen type III and loss of structural integrity can lead to reduced biomechanical strength of a diseased tendon – further exacerbating pain and loss of function. There is no curative treatment for chronic tendon disease primarily due to the absence of well-defined pathogenic pathways (Dakin *et al.*, 2017). Patients are left to manage their symptoms with analgesics, lifestyle changes, physical therapy and, ultimately, surgical procedures with limited efficacy. This unmet clinical need reflects the limited understanding of key pathogenic cell types and the underlying signalling mechanisms that underpin chronic tendinopathy. Recent studies suggest that chronic inflammation and dysregulated healing mechanisms play a central role in the pathophysiology of tendinopathy (Akbar *et al.* 2021; Dakin *et al.* 2017). Identifying key pathogenic and reparative tenocyte subpopulations will inform the design of tendon-disease models and accelerate the development of precision therapeutic strategies to cure tendinopathy.

The understanding of the cells and signalling pathways in diseased *versus* normal tendon is changing rapidly with next-generation sequencing techniques. It is only over the past 3 years that multiple discrete tendon cell subpopulations have been described in healthy and diseased human tendons using single-cell transcriptomics (Kendal *et al.*, 2020) as well as in murine tendons (De Micheli *et al.*, 2020; Giordani *et al.*, 2019; Harvey *et al.*, 2019; Tabula Muris *et al.*, 2018). Subsequent *in situ* transcriptomic analysis of human tendon tissue immediately *ex vivo* (Akbar *et al.*, 2021) supported the original single-cell

sequencing atlas (Kendal *et al.*, 2020) and argued the case for pro-inflammatory stromal-immune cell interactions in (shoulder) tendinopathy. As burgeoning tendon cell atlases provide greater insight into the pathogenesis of tendinopathy by identifying changes in tendon cell populations between healthy and diseased tissues, it is likely that the ability to identify, isolate and interrogate tendon cells of interest *in vitro* will be fundamental in developing bespoke precision treatments. Not only will differences between diseased *versus* healthy tenocyte gene expression highlight key pathogenic signalling pathways, but also the ability to identify and isolate healthy subpopulations that dominate normal tendon will enable focussing on *in vitro* design of implantable scaffolds that aid tendon repair and healing.

There are several important challenges in achieving a reliable assessment of normal tenocyte behaviour *in vitro*. Firstly, tendon cells are sparsely distributed and adherent to the dense surrounding extracellular matrix. Therefore, cell yield can be low and necessitates mechanical and enzymatic processing that could influence cell characteristics. Secondly, the previously described tendon cell subpopulations in mouse and human tendon, including most recently healthy *versus* diseased human tendon cells *in vitro* (Still *et al.*, 2021), are based on single-cell differential gene expression analysis. While there is some conservation between the species and overlap across different human tendon sites and different studies (Akbar *et al.*, 2021; De Micheli *et al.*, 2020; Giordani *et al.*, 2019; Kendal *et al.*, 2020), it remains possible that the described clusters are a product of confounding transcriptomic variation. Moreover, the first application of CITE-Seq to human tendon identified only a small number of cell-specific surface proteins and there is currently no optimal set of surface markers by which the various subsets can be identified (Kendal *et al.*, 2020). Therefore, it is unclear how differentiated or pluripotent cells are within a given cluster or if cells across several clusters share a common progenitor. Finally, tendon cells have been shown to be mechano-sensitive, changing their shape, migration, proliferation rate and gene expression profile in response to differing culture surfaces (Bashur *et al.*, 2009; Hakimi *et al.*, 2015; Kendal *et al.*, 2017; Lee *et al.*, 2005; Still *et al.*, 2021). Recreating the normal tendon architecture is likely a requisite condition for examining normal and diseased tendon cell behaviour *in vitro*. This will be particularly important when developing implantable scaffolds to improve tendon healing (Hakimi *et al.*, 2015; Nezhentsev *et al.*, 2021).

To overcome some of these challenges and determine whether human tenocyte subpopulations persist in different *in vitro* scaffold conditions, single-cell surface proteomics was combined with transcriptomics analysis using CITE-Seq. Hamstring-derived *in vitro* tenocyte subpopulations cultured for 8 d on either tissue culture plastic or electrospun PDO fibres were examined. PDO was selected as a comparator scaffold to tissue culture plastic as it has an established safety record as suture material and can be electrospun into fibres to mimic tendon architecture (Martins *et al.*, 2020; Mouthuy *et al.*, 2015). Despite previous demonstrations of electrospun PDO as a viable fibroblast scaffold material (Kendal *et al.*, 2017), it is unclear if all tendon fibroblast subtypes can attach and survive in this substrate or if only a few subsets are self-selected. The present study aimed to identify which tenocyte subpopulations preferentially adhered to these electrospun PDO fibres and proliferated in that environment.

Results demonstrated that multiple human tendon cell subtypes persisted *in vitro*, 4 of which shared transcriptomic and surface proteomic characteristics with *ex vivo* human tenocyte populations. 3 tenocyte populations preferentially survived on aligned electrospun PDO fibrous scaffolds (DCN_LUM, POSTN_SCX, and PTX3_PAPPA), upregulating TNF-α, IFN-γ, IL-6 and reparative matrix gene pathways. Additionally, the study identified surface markers that may be used to isolate and interrogate specific tenocyte subpopulations in future studies.

Materials and Methods

Tendon collection and cell processing

Tendon biopsies were collected from 6 patients after obtaining informed donor consent, in accordance with the Declaration of Helsinki, under ethics approval from the Oxford Musculoskeletal Biobank (09/H0606/11) and in compliance with National and Institutional ethical requirements. Only waste tissue that would otherwise have been disposed was collected. The age range of donors was 29-54 years, with a mean of 37 years. Samples were taken from 5 males and 1 female undergoing knee ligament reconstruction surgery following sports injuries. None of the donors suffered from diabetes mellitus, infection or inflammatory arthropathy. One hamstring tendon biopsy was obtained from each patient undergoing reconstruction of the knee anterior cruciate ligament. Tendon samples measuring 10 (length) × 10 (width) mm were excised distal to the myotendinous junction and proximal to the enthesis to ensure only mid-substance tendon was used. Samples were immediately placed in 4 °C Iscove's modified Dulbecco's medium without antibiotics and without FCS. The entire tendon (including the epitenon) was rinsed in 1× PBS, cut axially using a size 10 surgical scalpel into 1 mm^3 pieces and incubated at 37 °C for 45 min in 500 µm Liberase (Merck) medium supplemented with 10 µL/mL DNAse I (Thermo Scientific), as per previous protocol (Kendal *et al.*, 2019). Ham's F-12 medium + 10 % FCS was added and the digested tissue passed through a 100 µm cell strainer. Then, cells were passaged to passage 1 (P1) over 3-5 d using culture medium containing DMEM F12 medium (Lonza),

10 % FCS (Labtech, Uckfield, UK) and 1 % penicillin-streptomycin (Thermo Fisher Scientific) at 37 °C and 6 % CO_2. The culture medium was replaced every 3 d.

Fibrous scaffold preparation, cell seeding and cell culture

PDO fibres were electrospun using a modified version of a previously described protocol (Hakimi *et al.*, 2015). In brief, a 7 % w/v polymer solution of PDO (Riverpoint Medical, Portland, OR, USA) in HFIP (Halocarbon Product Corporation, North Augusta, SC, USA) was prepared, with a proprietary that changes the conductivity of the solvent. Polymer solution was supplied by a syringe pump (integrated within the IME electrospinning machine) at a flow rate of 0.8 mL/h. An IME electrospinner (IME Technologies, Spaarpot, the Netherlands) was used. PDO fibres were electrospun for up to 4 h at 21 °C, 30 % relative humidity, from a double nozzle setup at 9.0-9.6 kV with a distance of 20.0 cm between the nozzle and the grounded collector. Aligned fibres of 800-1,000 nm in diameter were produced by electrospinning onto the collector-a drum covered with aluminium foil, which was rotated at 2,000 rpm. Light microscopy confirmed a density of 35 to 45 fibres per 0.01 mm^2 and SEM of spun samples was used to verify the diameter of the PDO fibres, as per previous protocols (Kendal *et al.*, 2017). The electrospun PDO fibres were stored under vacuum desiccation for up to 3 months. Aligned electrospun PDO fibres were stretched and secured over the surface of a 24-well plate Cell Crown™ insert (Sigma-Aldrich) as previously described (Kendal *et al.*, 2017).

The whole construct was sterilised in 100 % ethanol for 60 min and rinsed 5 times in sterile 1× PBS. 5×10^5 (50 µL of 1×10^6 cells/mL) human tendon cells suspended in culture medium were seeded onto the PDO fibre CellCrown™ construct. Cells were allowed to adhere for 5 min before the CellCrown™ construct was inverted and firmly placed into a well of a 24-well plate containing culture medium. This ensured that all the cells in the 24 well plate were attached to the PDO aligned fibres and not in contact with the tissue culture plastic surface. Every 3 d, the culture medium was refreshed and each aligned PDO fibre CellCrown™ construct was transferred to a fresh 24 well plate. Technical triplets were performed for each biological sample. The control group consisted of 1×10^3 tendon cells, from the same donor, seeded directly onto 24 well plates.

The tendon cells in both groups (the control tissue culture plastic group and the aligned PDO electrospun fibres group) were cultured in culture medium containing DMEM F12 medium + 10 % FCS + 1 % penicillin/streptomycin at 37 °C and 6 % CO_2. The culture medium was replaced every 3 d and cells were cultured for 8 d.

Cell proliferation

Cell proliferation was quantified using alamarBlue® Assay, previously validated (Ahmed *et al.*, 1994; Voytik-Harbin *et al.*, 1998). On day 1, 4 and 7 of culture, the PDO fibre CellCrown™ constructs were transferred into fresh 24-well plates to exclude from the analysis any cells no longer attached to the PDO fibres. 10 % alamarBlue® (Invitrogen) in culture medium was added to the fresh wells containing the PDO fibre CellCrown™ constructs as well as the 24-well plate containing cells cultured on tissue culture plastic. In both groups, the cells were incubated at 37 °C for 4 h. 100 µL samples ($n = 3$) were taken from each of the wells and pipetted into a 96-well plate. Fluorescence was measured using a FLUOstar Omega Microplate Reader (BMG Labtech, Aylesbury, UK) at 544 nm excitation and 590 nm emission and compared to a cell density calibration curve of hamstring tenocytes cultured on a 24-well plate under the same conditions. Technical triplicates were performed for each biological sample.

CITE-seq

Cells were dissociated by incubation at 37 °C for 10 min using 500 µL per well of StemPro® Accutase® (Thermo Fisher). Tendon cells cultured on tissue culture plastic or PDO electrospun fibres were washed and re-suspended in 100 µL staining buffer (1× PBS + 2 % BSA + 0.01 % Tween-20). As per the CITE-Seq protocol (Web ref. 1), cells were incubated for 10 min at 4 °C in human Fc Blocking reagent (FcX, BioLegend). Cells were incubated at 4 °C for a further 30 min with 0.5 µg of TotalSeq-A (Biolegend) monoclonal anti-CD10 (312231), anti-CD105 (323221), anti-CD146 (361017), anti-CD26 (203720), anti-CD31 (102437), anti-CD34 (343537), anti-CD44 (338825), anti-CD45 (304064), anti-CD54, anti-CD55 (311317), anti-CD90 (THY1; 328135), anti-CD95 (305649), anti-CD73 (344031), anti-CD9 (312119) and anti-CD140a (323509) antibodies. These surface targets were selected based on TotalSeq-A workflow availability and their expression in cells populations from different lineages, including the endothelial, stromal and immune compartments. In addition, cells were incubated with 0.5 µg of 1 of 8 surface hashing antibodies (Biolegend) so that their sample of origin could be identified following sequencing across two lanes, as previously described (Kendal *et al.*, 2020).

Cells were washed 3 times with staining buffer and re-suspended in 1× PBS at 1,000 cells/µL. The cell suspensions were filtered using a 100 µm sieve. The final concentration, single cellularity and viability of the samples were confirmed using a haemocytometer. Cells were loaded into the Chromium controller (10× Genomics, Oxford, UK) chip following the standard protocol for the Chromium single cell 3' kit. A combined hashed cell concentration was used to obtain an expected number of captured cells between 5,000 and 10,000. All subsequent steps were performed based on the CITE-Seq protocol (Web ref. 2). Libraries were pooled and sequenced across multiple Illumina HiSeq 4000 lanes to obtain a read depth of approximately 30,000 reads per cell for gene expression libraries.

The raw single-cell sequencing data was mapped and quantified using the 10× Genomics Inc. software package CellRanger (v2.1) and the GRCh38 reference genome. Using the table of unique molecular identifiers produced by Cell Ranger, droplets that contained cells were identified using the call of functional droplets generated by Cell Ranger. After cell-containing droplets were identified, gene expression matrices were first filtered to remove cells with > 5 % mitochondrial genes, < 200 or > 5,000 genes and > 25,000 UMI. Downstream analysis of Cell Ranger matrices was carried out using R (3.6.0) and the Seurat package (v 3.0.2; Web ref. 3).

In total, 10,990 cells were selected for ongoing analysis after quality control filtering. Data were normalised using the SCTransform function for RNA gene expression, HTO and ADT expression level. Cells were selected based on the high expression level of their donor-specific surface hashing antibody and low expression level of the remaining hashing antibodies. Normalised data from all tendon cells were combined into one object and integrated. Variable genes were discovered using the SCtransform function with default parameters. The FindIntegrationAnchors function command used default parameters (dims = 1:30) to discover integration anchors across all samples. The IntegrateData function was run on the Anchorset, with additional default arguments. Then, ScaleData and RunPCA were performed on the integrated assay to compute 16 PC. UMAP dimensionality reduction was carried out and SNN graph was constructed using dimensions 1:16 as input features and default PCA reduction (Becht *et al.* 2018). Clustering was performed on the Integrated assay at a resolution of 0.5 with otherwise default parameters (Butler *et al.*, 2018).

Seurat FindAllMarkers was used to identify positive and negative markers of a single cluster compared to all other cells. Following expression level normalisation using SCTransform function, the average expression level of a feature (*e.g.* gene or surface protein) was calculated across each cluster. The minimum percentage of cells in which the feature is detected in each group was set to 25 %. The average Log2 fold change threshold was set to at least 1.0 such that the average expression level of a feature would have to be at least double in one cluster compared to another to reach the threshold. Significance was determined using Wilcoxon rank-sum test with *p*-values adjusted based on Bonferroni correction applying all features in the data set ($p\_val\_adj < 0.05$).

Gene-set enrichment analyses were performed using the R Bioconductor v3.13 package, with reference to Molecular Signatures Database v7.4 and Reactome Pathway Database.

R NicheNet was used to model cell-cell communication among cultured tenocytes by linking differential ligand gene expression to target gene expression. The method combines prior data of weighted signalling and gene regulatory network databases with cell expression data to predict ligand-receptor interactions (Browaeys *et al.*, 2020). NicheNet requires distinct cell types to be designated as "senders" and "receivers" in each simulation. A reference condition (in this case, tissue culture plastic) and a condition of interest (PDO fibrous scaffolds) in the gene expression data set are defined and used by the NicheNet algorithm to determine which genes are differentially expressed. To predict ligand-receptor interactions, NicheNet searches for receptors in the receiver cell types that can be affected by differentially expressed ligands in the sender cells. NicheNet further scores these ligand-receptor interactions by prioritising ligands with a high regulatory potential, as well as highlighting those ligands with the highest fold change in gene expression between the reference condition and condition of interest.

Results

scRNA-seq revealed multiple human tendon cell clusters *in vitro*

Healthy human hamstring tendon cells from 6 donor patients were split into two groups and cultured on either tissue culture plastic or electrospun aligned PDO fibrous scaffolds. After 8 d of culture, 10,990 human hamstring tendon cells underwent single-cell transcriptomic analysis post quality control. 2,765 of the cells analysed were from PDO fibre culture and 8,225 from tissue culture plastic. As in previous studies, cells proliferated at a significantly higher rate on tissue culture plastic, which accounted for the difference in cell numbers (Kendal *et al.*, 2017). Unsupervised graph-based clustering and UMAP (Becht *et al.*, 2018) of the integrated dataset (all cells cultured on tissue culture plastic and PDO fibres) revealed 7 transcriptomic clusters (Fig. 1). All 7 cell clusters were composed of cells expressing high levels of tenocyte-associated genes (including *COL1A1*, *COL1A2*, *COL3A1*, *FBLN*, *FBN1* and *ELN*) and low expression of genes associated with endothelial (*CD34*, *PECAM1*, *VWF*), immune (*IL7R*, *CD14*, *CD68*) or skeletal muscle (*MYF5*, *ACTA2*) cells (Fig. 1**d**). Dividing cells were identified by increased expression of cell cycle genes, including *MKI67*, *TOP2A* and *PCNA*. The top 15 differentially expressed genes for each cluster are summarised in Fig. 1**e**. PTX3_PAPPA and DCN_LUM clusters were predominantly composed of cells cultured on aligned PDO fibres. Most DKK1_FGF5, PTX3_PAPPA, POSTN_SCX and PRELP_FMOD cluster cells were cultured on tissue culture plastic (Fig. 1).

To help further define the clusters observed *in vitro*, expression of the top 20 differentiating genes previously found in the dataset of *ex vivo* human tendon clusters (Kendal *et al.*, 2020) was analysed for each *in vitro* cluster (Fig. 2**a**). *In vitro* ITGA7_NES cells demonstrated expression of genes found in *ex vivo* ITGA7+ cells. *In vitro* PTX3_PAPPA cells demonstrated increased expression of genes found in *ex vivo* PTX3+ cells. *In vitro* DCN_LUM cells

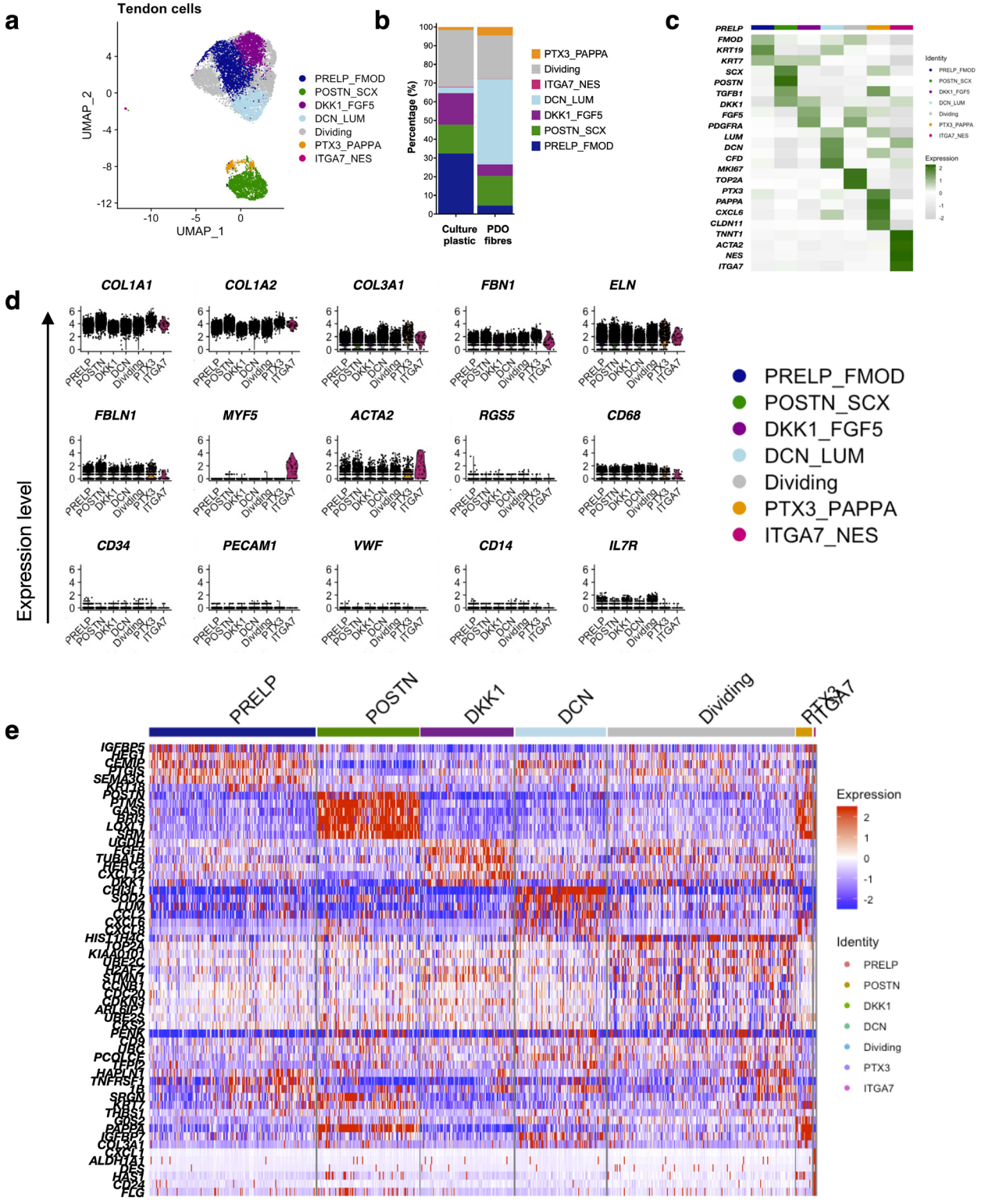

Fig. 1. Single-cell atlas of cultured human hamstring tendon cells. (**a**) Single-cell transcriptomic UMAP dimensionality reduction of cultured human hamstring cells revealed 6 discrete cell clusters. The data represents 10,990 cells; 2,765 cultured on PDO fibres and 8,225 cultured on tissue culture plastic for 8 d. (**b**) Proportion of clustered cells cultured on tissue culture plastic and PDO fibres. (**c**) Heatmap of average expression of top 3 differentiating genes per cluster. (**d**) Violin plots show high expression of matrix genes *COL1A1*, *COL1A2*, *COL3A1*, *FBN1*, *ELN* and *FBLN1* in all clusters. (**e**) Heatmap demonstrating relative expression level of top 15 genes in each cluster.

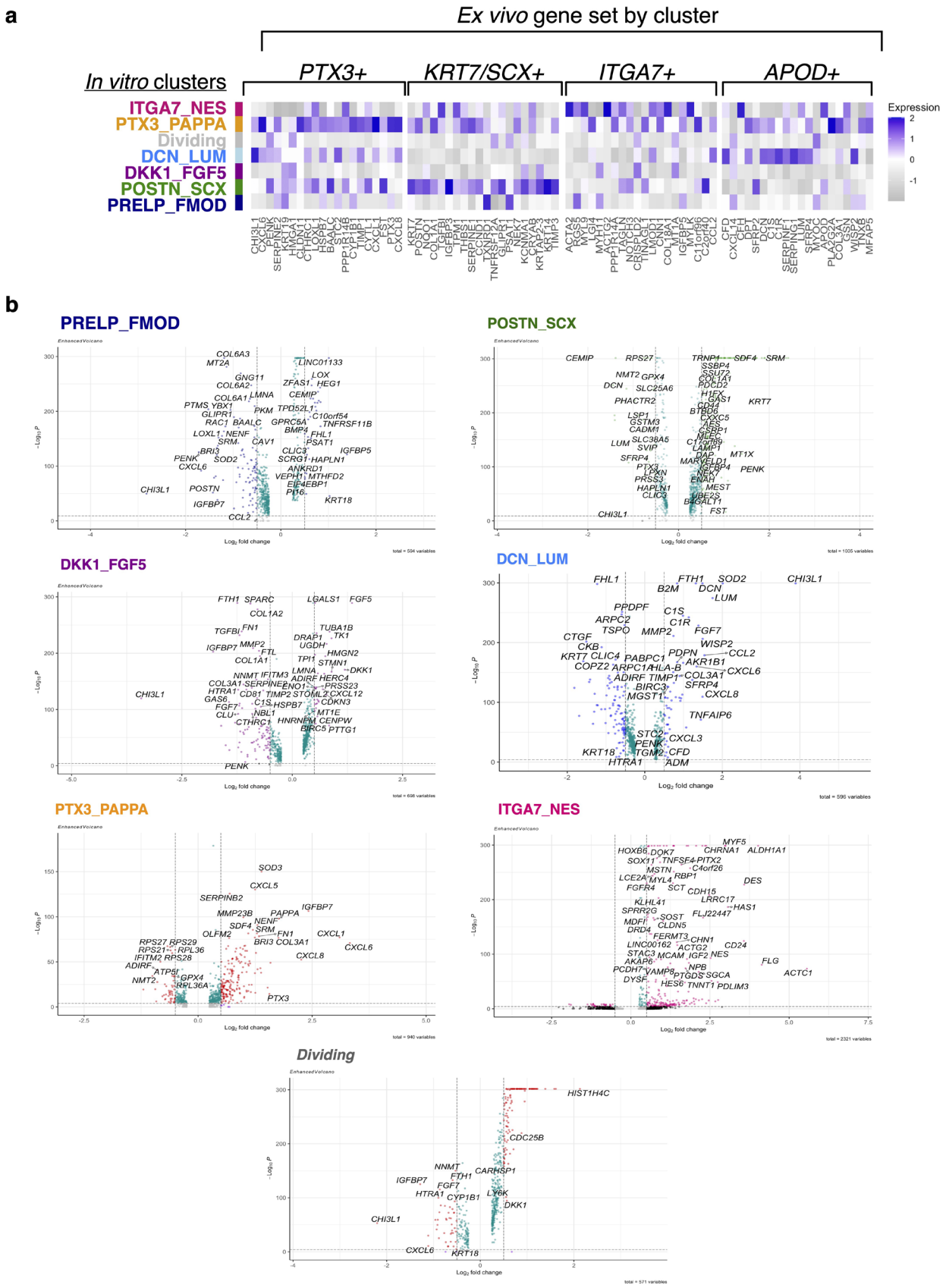

Fig. 2. Differential gene expression of hamstring cells cultured *in vitro*. Data represent the integrated set of 10,990 cells cultured on either tissue culture plastic or aligned PDO fibres. (**a**) Heatmap showing the relative average expression for each *in vitro* cluster (Y axis) of the top 20 genes previously found to be expressed by *ex vivo* human tendon cell clusters (X axis, historical dataset). (**b**) Volcano plots of differential genes expression for each *in vitro* cluster (labelled genes > 0.5 Log2-fold change in expression, $p < 0.001$).

demonstrated increased expression of genes found in *ex vivo* APOD+ cells. *In vitro* POSTN_SCX cells demonstrated increased expression of genes found in *ex vivo* KRT7/SCX+ cells (Fig. 2**a**). Fig. 2**b** shows the top differentially expressed genes for each *in vitro* cluster with reference to the remaining clusters (labelled genes indicating those expressed at > 0.5 Log2 fold change, $p < 0.001$).

CITE-Seq surface proteomic analysis was performed using Total-SeqA (Biolegend) oligonucleotide-conjugated monoclonal antibodies against 12 cell surface protein markers (Fig. 3). This revealed that PTX3_PAPPA cells expressed high levels of surface CD10, CD26 and CD54 proteins. CD146 protein was upregulated on the cell surface of ITGA7_NES cluster cells. POSTN_SCX cells were CD90+CD95+CD10+. PRELP_FMOD cells were CD90low and CD10neg. Low surface expression of CD10, CD26 and CD54 proteins was observed on cells in the DCN_LUM cluster. DKK1_FGF5 cluster cells did not express high levels of any surface proteins targeted in the present study.

Characteristics of cells preferentially cultured on aligned PDO electrospun fibres

The cells grown on PDO electrospun fibres proliferated but at a significantly lower rate compared to cells cultured on plastic over 8 d (Fig. 4**a**, mean 1.7-fold increase *versus* 5.1-fold increase in cell numbers respectively, $p < 0.001$). There was no significant difference in the expression of *COL1A1*, *COL1A2*, *COL3A1*, *FBN1*, *ELN* and *FBLN1* between cells cultured on PDO fibres *versus* tissue culture plastic (Fig. 4**b**, grey *versus* white, respectively). Split violin plots demonstrated that comparable levels of surface CD10, CD26, CD54, CD90, CD95 and CD105 were seen for cells cultured on tissue culture plastic and electrospun PDO fibres across all clusters (Fig. 4**c**). CD146 surface-protein expression was higher in ITGA7_NES cluster cells cultured on plastic as compared to PDO electrospun fibres, but very few ITGA7_NES cells survived on PDO fibres (Fig. 1**b**, 4**c**).

DCN_LUM, POSTN_SCX and PTX3_PAPPA cells preferentially survived on PDO electrospun scaffolds (Fig.1**b**). In these 3 clusters, significantly higher expression of *SOD2*, *CXCL1*, *CXCL6* and *CXCL8* was observed in cells cultured on PDO electrospun fibres *versus* tissue culture plastic (Log2 fold change > 0.5, $p < 0.05$; Fig. 5**a**). *COL6A3* was significantly increased in cells from PRELP_FMOD, DCN_LUM, PTX3_PAPPA and DKK1_FGF5 clusters when cultured on PDO electrospun fibres *versus* tissue culture plastic. *COL3A1* expression was increased in DCN_LUM and PRELP_FMOD cells cultured on PDO electrospun fibres. PRELP_FMOD cells additionally demonstrated increased expression of *COL8A1*, *DCN*, *FN1*, *LUM* and *MMP2* when cultured on PDO electrospun fibres.

Gene Ontology mapping was undertaken for differentially expressed genes observed in cells cultured on electrospun PDO fibres compared to tissue culture plastic (Fig. 5**b**). Hallmark gene set enrichment analysis was performed with reference to the Molecular Signatures Database of 50 well defined

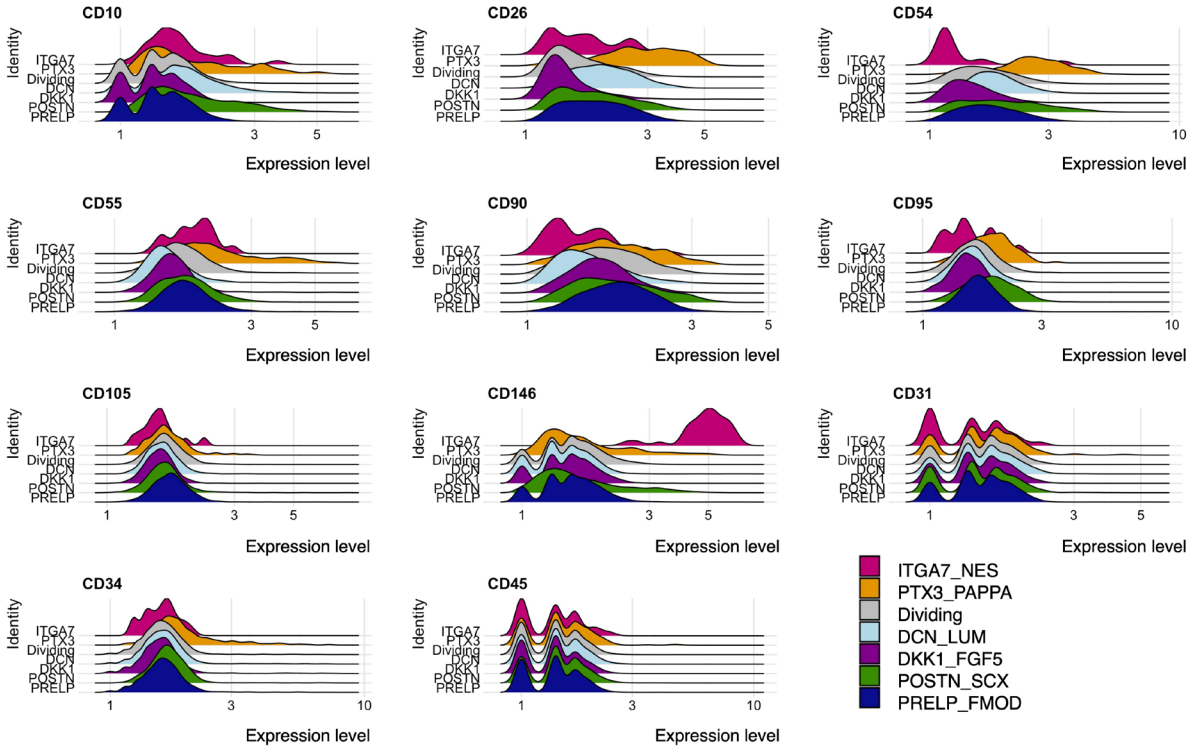

Fig. 3. CITE-seq differential surface protein expression of hamstring cells cultured *in vitro*. Data represent the integrated set of 10,990 cells cultured on either tissue culture plastic or aligned PDO fibres. Ridgeplots of surface proteins detected by oligonucleotide-conjugated anti-CD10, anti-CD26, anti-CD54, anti-CD55, anti-CD90, anti-CD95, anti-CD105, anti-CD146, anti-CD31, anti-CD34 and anti-CD45 for each cell cluster of the integrated dataset.

biological processes and the Reactome Pathway Database. Culturing human hamstring tendon cells on PDO electrospun fibres upregulated gene sets associated with the "TNF-α signalling *via* NF-κB" and "Inflammatory response" categories in all clusters. An increase in genes associated with the "IFN-γ signalling" category was observed for cells cultured on PDO electrospun fibres from all clusters except POSTN_SCX. IL-6/STAT3 signalling was increased in POSTN_SCX, DCN_LUM and PTX3_PAPPA clusters (Fig. 5**b**). A corresponding reduction in expression of genes associated with the "Hallmark myogenesis" category was observed in ITGA7_NES, POSTN_SCX and PTX3_PAPPA cluster cells cultured on PDO electrospun fibres compared with those from tissue culture plastic.

Cell selection based on surface protein expression

CITE-Seq single-cell surface proteomics allowed cells to be selected from the integrated dataset based on

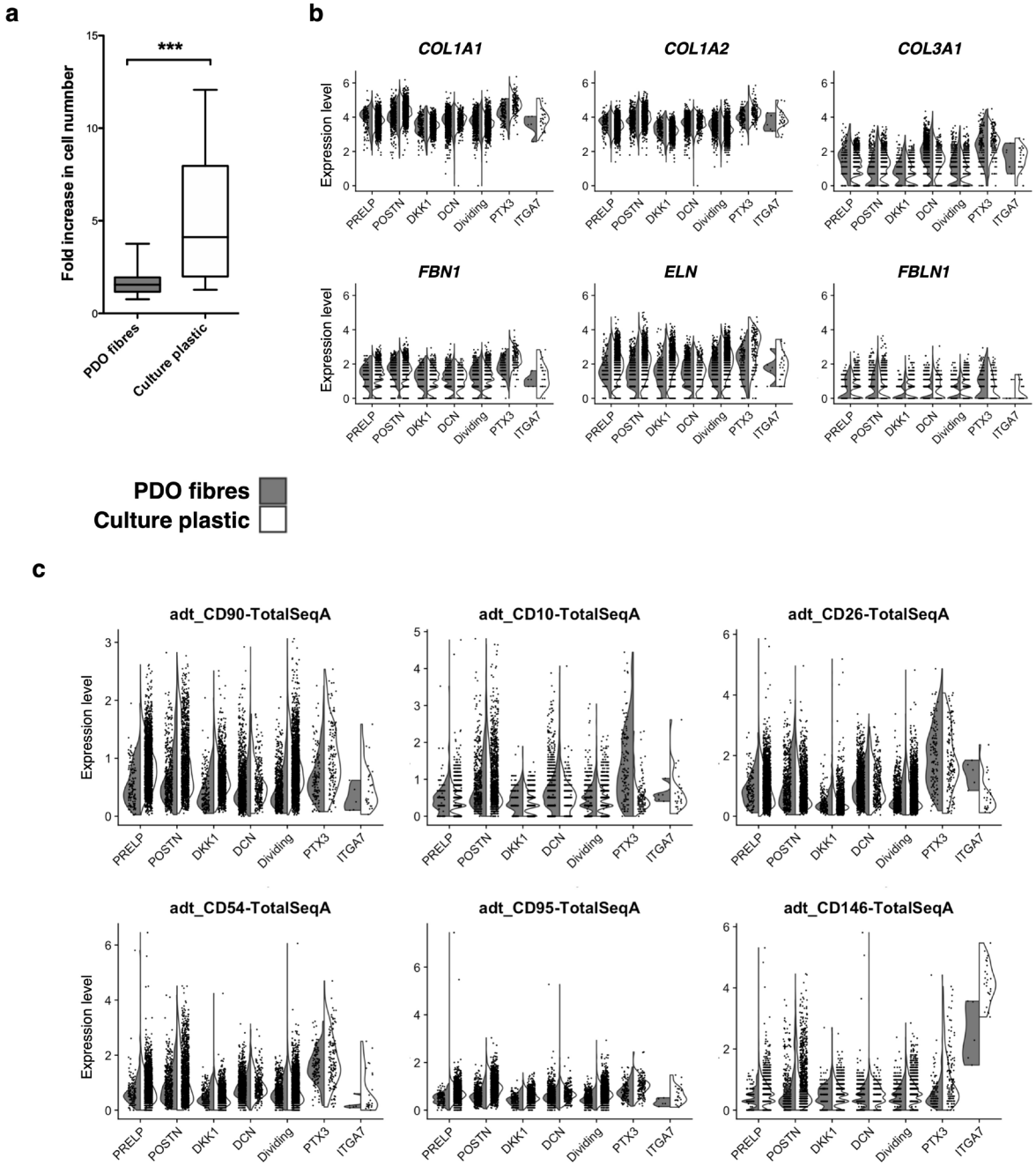

Fig. 4. Human tendon cells cultured on tissue culture plastic *vs.* PDO fibres. (**a**) Cells cultured on tissue culture plastic proliferated at significantly higher rate than those on PDO fibres (5.1 *versus* 1.7-fold increase over 7 d respectively, $p < 0.001$). (**b**) Split violin plots showed there was no significant difference in expression of matrix genes *COL1A1*, *COL1A2*, *COL3A1*, *FBN1*, *ELN* and *FBLN1* between cells on PDO fibres (grey) and tissue culture plastic (white). (**c**) Split violin plots of oligonucleotide-conjugated monoclonal antibody recognising surface proteins show no significant difference in surface CD90, CD10, CD26, CD54, and CD95 expression between cells on PDO fibres (grey) *versus* tissue culture plastic (white). Very few ITGA7_NES cells survived on PDO fibres and had reduced surface CD147 expression.

surface protein expression before performing further single-cell gene expression analysis. In this way, cells were segregated into groups based on high expression levels of surface protein CD10, CD26, CD54, CD90, CD95, CD105 or CD146. Differential gene expression of cells cultured on PDO electrospun fibres *versus* plastic was analysed for each group (Fig. 6). An increase in TNF-α signalling gene sets was observed for CD26+CD54+CD90+CD95+CD105+CD146+ cells cultured on PDO electrospun fibres (Fig. 6). CD10+ cells cultured on PDO electrospun fibres upregulated gene sets associated with the "INF-γ response", "TNF-α signalling" and "Chemokine receptor binding chemokines" categories (Fig. 6**e**). In comparison, gene sets associated with myogenesis were downregulated *versus* cells cultured on plastic

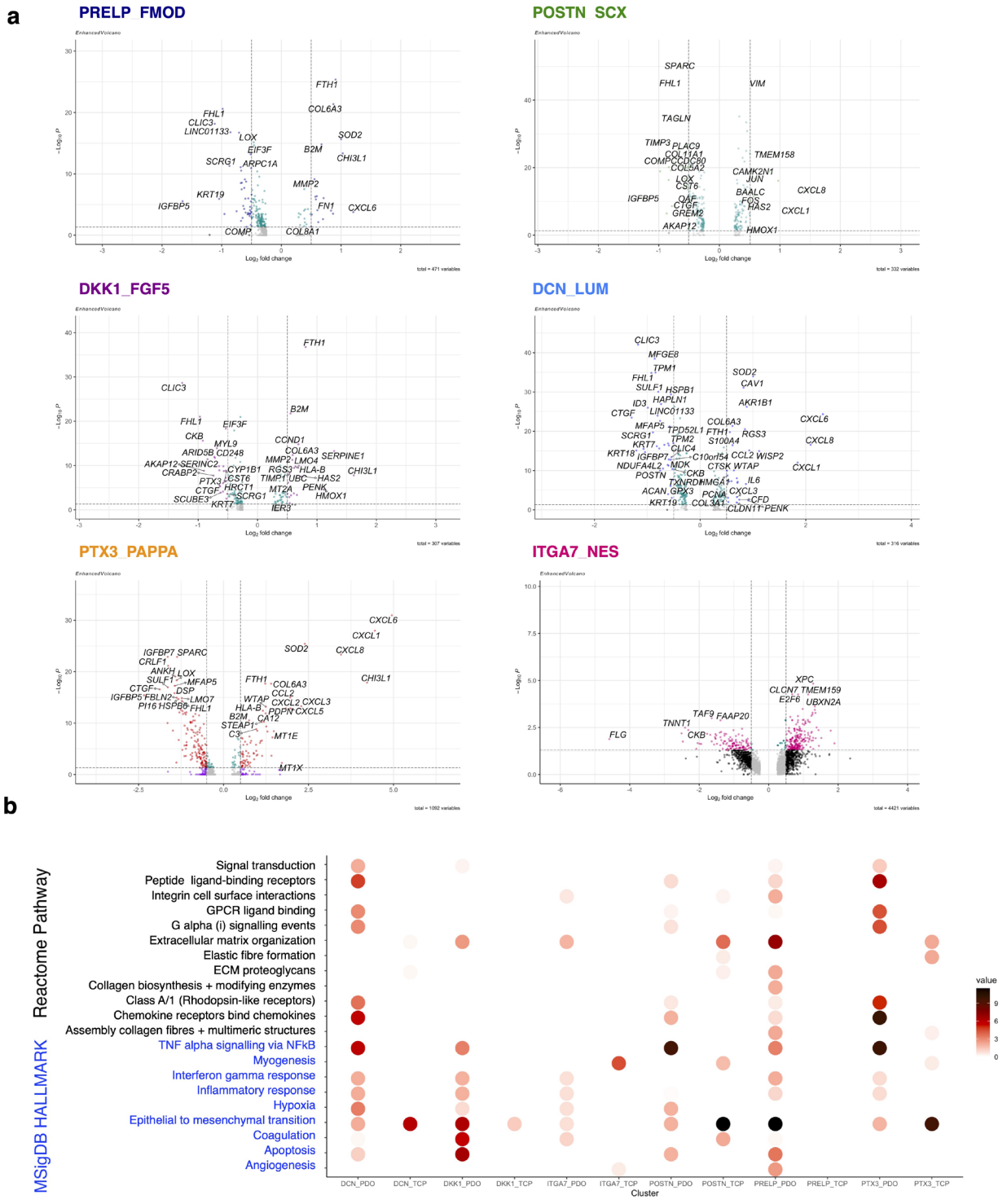

Fig. 5. Differential gene expression of hamstring cells cultured on PDO fibres *versus* culture plastic. (**a**) Volcano plots of differential gene expression on PDO fibres *versus* tissue culture plastic for each *in vitro* cluster (labelled genes > 0.5 Log2-fold change in expression, $p < 0.001$). (**b**) Gene Ontology enrichment analysis of gene sets upregulated in each cluster when cultured on PDO fibres (_PDO) *versus* tissue culture plastic (TCP-labelled X axis) with reference to Reactome Pathway and MSigDB Hallmark databases (Y axis).

alone. The "Hallmark IL-6_JAK_STAT" signalling gene expression category was increased in both CD54+ and CD90+ cells on electrospun PDO fibres. CD90+ cells, CD95+ cells and CD105+ cells cultured on PDO fibres upregulated genes associated with IFN-γ signalling. Gene sets associated with extracellular matrix production pathways, including "Epithelial to mesenchymal transition", "Extracellular matrix organisation" and "Collagen formation" categories, were increased in CD26+ cells, CD54+ cells, CD90+ cells, CD95+ cells and CD105+ cells when cultured on PDO fibres. In contrast, CD146+ cells cultured on electrospun PDO fibres had downregulated expression of the "Epithelial to mesenchymal transition" and "Extracellular matrix organisation" categories gene sets compared to those cultured on tissue culture plastic (Fig. 6**b**).

Cells that were selected based on the combined surface expression of CD10+, CD26+ and CD54+ exhibited increased expression of genes belonging to the "Hallmark TNF-α signalling", "INF-γ response" and "Inflammatory response" categories when cultured on aligned PDO fibres. They had also upregulated expression of genes associated with the "Chemokine receptors bind chemokines", "Degradation of extracellular matrix", "Activation of matrix metalloproteinases" and "Extracellular matrix organisation" categories (Fig. 6**h**). Genes belonging to the "Hallmark myogenesis" category were downregulated in culture with aligned PDO fibres *versus* tissue culture plastic.

Intercellular communication between clusters

NicheNet analysis of predicted intercellular interactions among the tenocyte clusters was performed for cells cultured on electrospun PDO fibres *versus* tissue culture plastic (Browaeys *et al.*, 2020). Cells in each cluster were designated as senders and cells in the remaining clusters as receivers. Then, ligand-receptor interaction was modelled by searching for receptor genes in the receiver cell types that were affected by differentially expressed ligands in the sender cell types. Potential interactions were referenced to signalling and gene regulatory network databases, including intracellular signalling networks. Tissue culture plastic was defined as the reference condition and compared against cells cultured on PDO fibrous scaffolds.

Fig. 7**a** shows predicted interactions of PTX3_PAPPA cells as receivers with PRELP_FMOD sender cells *via* the *TGFB1* and *EDN* pathways, both of which were upregulated when cells were cultured on PDO fibres. PTX3_PAPPA interaction with ITGA7_NES and DKK1_FGF5 clusters *via TGFB1* pathway was observed and was downregulated during PDO fibre culture. FGF1 pathway signalling in PTX3_PAPPA receiver cells from POSTN_SCX, DKK1_FGF5 and ITGA7_NES clusters was also downregulated on PDO fibre culture *vs.* tissue culture plastic.

POSTN_SCX, as receiver cells, interacted with PRELP_FMOD sender cells *via* upregulation of *TGFB1* during PDO fibre culture (Fig. 7**b**). *NAMPT* and *VEGFA* signalling from PTX3_PAPPA to POSTN_SCX cells was increased in cells cultured on electrospun PDO fibres, with a marked increase in signalling from PTX3_PAPPA sender cells *via NAMPT*. Conversely, the interaction of POSTN_SCX cells with ITGA7_NES, DCN_LUM and DKK1_FGF5 sender cells *via TGFB1* was downregulated on electrospun PDO fibres. *FGF1* pathway signalling in all sender cell types was also downregulated on electrospun PDO fibres.

NicheNet inferred that DKK1_FGF5 receiver cell signalling *via* the *CTGF* pathway was downregulated in all sender cell types and particularly in the PTX3_PAPPA cluster, during culture on electrospun PDO fibres (Fig. 7**c**). Similarly, there was a decrease in *TGFB1* signalling in DCN_LUM and ITGA7_NES sender cells and an increase in PRELP_FMOD sender cells. An upregulation of *HAS2* signalling was observed in all sender cell types except ITGA7_NES cells when cultured on electrospun PDO fibres.

Compared to tissue culture plastic, all cells cultured on electrospun fibres had downregulated signalling *via CTGF* in relation to receiver DCN_LUM cells (Fig. 7**d**). There were mixed observations of predicted *CXCL12* signalling pathways during culture on electrospun PDO fibres. Signalling was increased in relation to PRELP_FMOD, PTX3_PAPPA and ITGA7_NES sender cells but was downregulated in POSTN_SCX and DKK1_FGF5 cells. *NAMPT* pathway signalling was slightly increased in all cell types except for the DKK1_FGF5 cluster when cultured on electrospun PDO fibres. Predicted signalling *via* the *HAS2* pathway was also upregulated during PDO fibre culture in all cell types except ITGA7_NES cells, where signalling was downregulated.

An increase in predicted signalling *via PLAU* in ITGA7_NES and PTX3_PAPPA sender cells in relation to receiver PRELP_FMOD cells was observed during culture on electrospun PDO fibres (Fig. 7**e**). *WNT5A* signalling was increased in PTX3_PAPPA, ITGA7_NES and DKK1_FGF5 sender cells. There was also an upregulation of *VEGF* signalling by DKK1_FGF5 cells and a reduction in *TGFB3* signalling in POSTN_SCX and ITGA7_NES sender cells.

Lastly, NicheNet inferred that signalling *via HMGB1* and *HMGB2* increased in all sender cell types (except *HMGB2* in ITGA7 cells) in relation to dividing cells (receivers) during culture on electrospun PDO fibres (Fig. 7**f**). Additionally, there was also an increase in signalling *via HAS2* in DKK1_FGF5, POSTN_SCX and PTX3 sender cells. *TGFB1* signalling decreased in all sender cell types during culture.

Discussion

The study aimed to use surface markers expression and single-cell transcriptomic analysis to identify

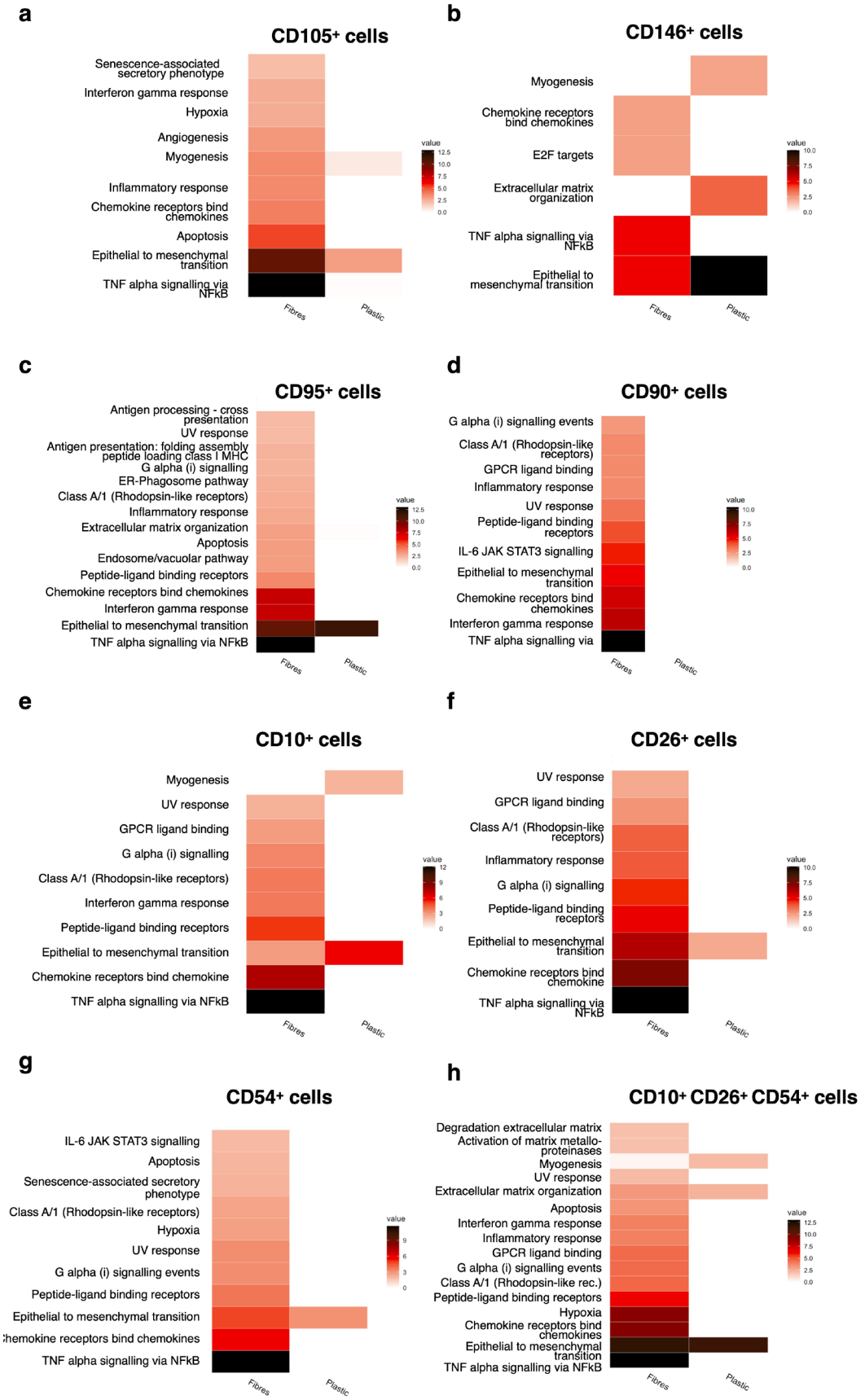

Fig. 6. Gene Ontology enrichment analysis of pre-selected hamstring cells cultured on PDO fibres *versus* culture plastic. Tendon cells were selected based on surface expression of (**a**) CD105, (**b**) CD146, (**c**) CD95, (**d**) CD90, (**e**) CD10, (**f**) CD26, (**g**) CD54 and (**h**) CD10+ CD26+ CD54+ proteins from the combined *in vitro* dataset. Gene Ontology enrichment analysis of differential gene expression was performed for each selected group of cells cultured on PDO fibres *versus* tissue culture plastic. Reactome Pathway and MSigDB Hallmark databases were used for reference.

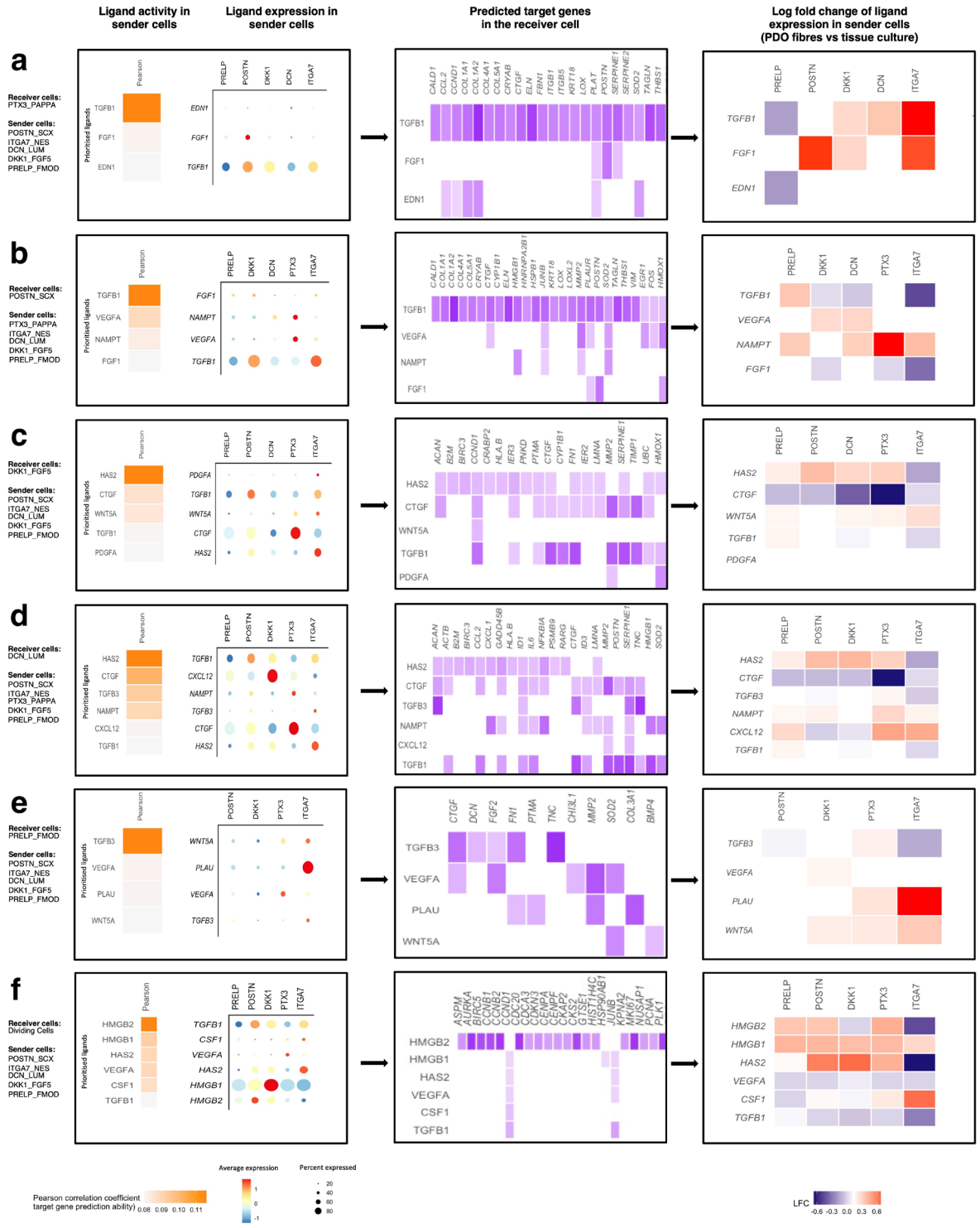

Fig. 7. Cell-cell interaction analysis of in vitro tenocytes cultured on tissue culture plastic versus PDO fibres. Each tenocyte population was compared against the rest to map all predicted ligand-receptor interactions. Culture plastic was set as reference condition and how cell-cell interactions changed compared to cells cultured on PDO fibres was explored. The first column in each receiver and sender cell combination represents the identified ligand activity for differentially expressed ligands and their average expression in the sender cells, the second column the predicted target genes and receptors in the receiver cells and the third column the Log-fold change in average expression when cells were cultured on PDO fibres *versus* tissue culture plastic. ITGA7_NES cells were excluded as receivers in this ligand-interaction analysis, as it was not possible to identify differentially expressed receptors in their expression profiles that interacted with other cell types' ligands.

human tendon cell subpopulations *in vitro*, comparing tenocytes grown on tissue culture plastic to the same cells grown on an aligned electrospun PDO fibrous scaffold. Single-cell RNA sequencing and cell proteomics of human hamstring tendon cells showed that multiple discrete cell clusters persisted in *in vitro* culture on tissue culture plastic and aligned PDO electrospun fibres. 6 main subpopulations were identified: PRELP_FMOD, POSTN_KRT7, DKK1_FGF5, DCN_LUM, PTX3_PAPPA and ITGA7_NES cells. All cell clusters expressed high levels of *COL1A1*, *COL1A2*, *COL3A1*, *ELN* and *FBLN1* associated with normal tendon matrix proteome (Hakimi *et al.*, 2017). In comparison to initial (Kendal *et al.*, 2019; 2020) and subsequent (Akbar *et al.*, 2021) *ex vivo* human tendon single-cell atlases, endothelial cells, monocytes and lymphocytes were not present after 8 d of culture under conditions that favoured tendon fibroblasts.

4 *in vitro* cell clusters shared gene expression profiles with *ex vivo* cell populations from a previous human tendon atlas (Kendal *et al.*, 2020), as shown in Fig. 2**a**. *In vitro* POSTN_KRT7, PTX3_PAPPA, ITGA7_NES and DCN_LUM clusters showed increased expression of the top differentially expressed genes initially found in the *ex vivo* POSTN+, PTX3+, ITGA7+ and APOD+ clusters, respectively. This supported the possibility that human tendon cell clusters represented populations that can be isolated *ex vivo* and remain discrete subtypes *in vitro* (Still *et al.*, 2021). There was little in the gene expression profile of cultured DKK1_FGF5 and PRELP_FMOD to relate them to cell clusters found in the *ex vivo* atlas. These 2 clusters might represent confounding variation, particularly batch variation or transient states of less well-differentiated tendon cells selected by particular *in vitro* culture conditions. Additionally, the *in vitro* clusters were derived from hamstring tendons, whereas the *ex vivo* atlas (Kendal *et al.*, 2020) analysed human tendons from various anatomical sites, which could produce different clustering results given the specific mechanical properties of distinct tendon types. Interestingly, 4 conserved cell clusters were observed, despite cross-referencing the *in vitro* dataset with a heterogeneous *ex vivo* dataset (Kendal *et al.*, 2020) with very little in common: different patient demographics, different anatomical tendons sampled and a combination of healthy and diseased tendons. These clustering results supported the existence of discrete human tendon cell populations.

The ability to identify cell populations by specific surface markers is essential for isolating live cells from each cluster (Cappellesso-Fleury *et al.*, 2010; Halfon *et al.*, 2011; Mohanty *et al.*, 2014). CITE-seq proteomics revealed that surface markers for 2 *in vitro* clusters, ITGA7_NES and PTX3_PAPPA, were consistent with previous *ex vivo* findings. Human ITGA7+ cells *ex vivo* had high CD146 surface expression (Kendal *et al.*, 2020), as did the cluster of *in vitro* ITGA7_NES cells (Fig. 3). PTX3+ cells are CD10+CD26+CD54+ *ex vivo* (Kendal *et al.*, 2020); similarly, PTX3_PAPPA cells were also CD10+CD26+CD54+ whether cultured on tissue culture plastic or PDO electrospun fibres. This was not the case for the other two clusters. POSTN_KRT7 cells *in vitro* were CD90+CD95+CD10+, whereas POSTN+ *ex vivo* cells were CD90+CD105+CD146+ and DCN_LUM cluster cells *in vitro* had low surface expression of CD10, CD26 and CD54 compared to APOD+ cells *ex vivo*, which were CD90+CD34+ (Fig. 3).

ITGA7_NES cells were first described in murine muscle as smooth-muscle mesenchymal cells situated in perivascular regions (Giordani *et al.*, 2019; Yin *et al.*, 2016). They express ACTA2, RGS5, MYL9 and TAGLN in murine tendon cells *ex vivo* (Giordani *et al.*, 2019; Yin *et al.*, 2016) as well as in human tendon cells *ex vivo* (Kendal *et al.*, 2020). The present study showed those markers' expression also in human tendon cells *in vitro*. Similarly to previous studies in which ITGA7+ (Kendal *et al.*, 2020) or *NES*+ cells were expanded on tissue culture plastic (Yin *et al.*, 2016), ITGA7_NES cells preferentially grew on tissue culture plastic and very few survived on PDO electrospun fibres (Fig. 1**b**). Those that did had reduced expression of hallmark genes associated with myogenesis and an increase in genes belonging to the "Epithelial to mesenchymal transition" and "IFN-γ response" categories (Fig. 5). It is important to note that ITGA7_NES cells expressed genes characteristic of both mural (*RGS5* and *ACTA2*) and fibroblast (*COL1A1/2* and *COL3A1*) cells. This discrepancy highlights the ambiguity of canonical fibroblast markers and raises questions about the identity of mural cells, smooth-muscle mesenchymal cells and fibroblasts in tendon. These mural-like fibroblasts in tendon have been reported in human and mouse single-cell studies (Giordani *et al.*, 2019; Kendal *et al.*, 2020) but no standard nomenclature has been established for them.

PTX3+ cells from chronic diseased tendon have previously been shown *ex vivo* to upregulate *CHI3L*, *CLDN11*, *PENK*, *SERPINE2* and pro-inflammatory genes such as *CXCL1*, *CXCL6* and *CXCL8*, suggesting they may play a role in driving inflammation in chronic tendinopathy (Kendal *et al.*, 2020). *In vitro* PTX3_PAPPA cells preferentially survived as well as proliferated on aligned PDO electrospun fibres (Fig. 1**b**) and presented increased expression of *CHI3L*, *CXCL1*, *CXCL3*, *CXCL6* and *CXCL8* (Fig. 5). Similarly, selecting *PTX3*-expressing cultured cells based on combined surface expression of CD10+, CD26+ and CD54+ showed increased expression of genes associated with TNF-α, INF-γ and G-coupled chemokine signalling pathways (Fig. 6**h**). The increased expression of genes belonging to the "Matrix metalloproteinases" category as observed in CD10+CD26+CD54+ cells on aligned PDO fibres suggested that *PTX3*+ cells may be involved in the early response to tendon disruption: recruiting immune cells and degrading abnormal tendon matrix to perform the groundwork for the next phases of tendon repair.

It is unclear from these very early findings if *PTX3*-expressing tenocytes were responding to a loss of tendon homeostasis by upregulating pro-inflammatory genes in an attempt to resolve micro-structural damage or if they were inappropriately driving chronic inflammation. These results suggested that aligned electrospun PDO fibres provided a useful scaffold and environment for their ongoing investigation *in vitro*. A similar population of cells expressing *IL8*, *CXCL1/6/8* and *PTX3* was described in single-cell transcriptomics of healthy and diseased patellar tendon progenitor cells cultured under mechanical stress (Still *et al.*, 2021). Most of these named "pro-inflammatory tendon progenitor cells" were from diseased human tendon and expressed gene sets enriched for pro-inflammatory signalling pathways, including the "IL-1 regulation of extracellular matrix" category. These complementary *ex vivo* and now *in vitro* findings add to the increasing evidence supporting pro-inflammatory tendon fibroblasts driving chronic tendon disease, possibly in response to a loss of normal tendon homeostasis (Akbar *et al.*, 2021; Dakin *et al.*, 2018). Focusing on a particular tendon cell subsets will advance the understanding of how tenocytes interact with immune cells (Garcia-Melchor *et al.*, 2021; Stolk *et al.*, 2017). It is now possible to isolate (based on CD10+, CD26+ and CD54+ surface markers) and to culture (PDO aligned fibres) *PTX3+* cells implicated in chronic human tendinopathy.

In general, cells proliferated at a slower rate on aligned PDO fibres compared to tissue culture plastic. This is consistent with previous observations (Kendal *et al.*, 2017). Tendon fibroblasts undergo a dramatic change in their morphology when seeded onto electrospun fibres, spreading along and across aligned fibres and using them as a scaffold on which to migrate (Hakimi *et al.*, 2015; Kendal *et al.*, 2017). The mechano-sensitivity of tendon cells to their surface environment is not restricted to electrospun fibres and is well documented on multiple structures (Bashur *et al.*, 2009; Fleischer *et al.*, 2015; Gomes *et al.*, 2015; Kim *et al.*, 2009; Lee *et al.*, 2005; Smith *et al.*, 2016). Historically, it has not been clear which tendon cells are more likely to adhere to the fibres, which preferentially survive and whether there are transcriptional and phenotypic differences in the responses of different subtypes. In the present study, 3 cell clusters preferentially survived on PDO electrospun fibres: DCN_LUM, PTX3_PAPPA and POSTN_SCX (Fig. 1**b**). These cells proliferated on PDO electrospun fibres and continued to express *COL1A1*, *COL1A2*, *COL3A1*, *FBN1*, *FBLN1* and *ELN* at similar levels to cells cultured on tissue culture plastic (Fig. 4**b**).

Gene enrichment analysis of the 3 clusters that proliferate preferentially on PDO fibres (DCN_LUM, PTX3_PAPPA and POSTN_SCX) revealed an upregulation of hallmark gene sets for the "TNF-α signalling *via* NF-κB" and "IL6_JAK_STAT6" categories (Fig. 5**b**). DCN_LUM and PTX3_PAPPA cells had upregulated expression of hallmark genes sets belonging to the "IFN-γ signalling" category. There was a relative reduction in the expression of genes associated with epithelial to mesenchymal transition in all 3 clusters. A similar upregulation in IL6-JAK-STAT3 signalling and TNF-α signalling *via* NF-κB is observed when hamstring tendon cells are cultured for 14 d on twisted electrospun PDO compared to tissue culture plastic and smooth PDS II (Nezhentsev *et al.*, 2021). Gene enrichment for Mtorc1 signalling was also upregulated, while gene sets associated with epithelial-to-mesenchymal transition were downregulated. Again, it is not clear if the observed pro-inflammatory signalling is a desirable early response to tendon damage and represents a favourable state when designing and screening implantable scaffolds to treat chronic tendinopathy.

Ligand-receptor analysis showed that *CTGF*, *VEGF* and *FGF1* interactions were downregulated in cells cultured on PDO fibres culture across all clusters. *TGFB1* signalling was also downregulated in all clusters, except PRELP_FMOD cells, during PDO fibre culture (Fig. 4**a**). These ligand-interaction analyses, and the lower growth rate of fibroblasts on PDO fibres, were consistent with previous studies showing that low expression of *TGFB1*, *CTGF*, *VEGF* and *FGF1* is associated with decreased cell proliferation and suppressed accumulation of fibroblasts and mural-associated cells in tendon tissue (Molloy *et al.*, 2003; Sakai *et al.*, 2017; Yun *et al.*, 2007). This intercellular interaction analysis forms the foundation for further investigation of requisite signalling in tendon regeneration and informs the design of scaffolds in studying tenocytes *in vitro*.

In the absence of defined surface markers by which cells of interest can be manually selected *in vitro*, CITE-Seq allows for transcriptomic analysis of cells virtually pre-selected based on high expression of a given surface marker. Split Violin graphs of surface protein expression demonstrated that there was no significant decrease in surface expression of CD90, CD10, CD26, CD54 and CD95 in cells cultured on aligned PDO electrospun fibres *versus* tissue culture plastic (Fig. 4**c**). Therefore, it was possible to select cells from the integrated dataset that have high surface expression of these proteins. Genes associated with inflammatory response and/or pro-inflammatory signalling pathways were seen in CD90+, CD10+, CD26+, CD54+, CD95+ and CD105+ cells cultured on PDO fibres (Fig. 6). CD146+ cells (which were predominantly ITGA7_NES cells) showed downregulated expression of hallmark genes belonging to the "Myogenesis", "Extracellular matrix organisation" and "Epithelial to mesenchymal transition" categories (Fig. 6**g**).

The study focused on a small set of surface proteins and future studies will greatly benefit from expanding their repertoire. In addition, it was not possible to identify and isolate tendon cell populations of interest, with the notable exceptions of immune cells, endothelial cells, *ITGA7/NES-* and

PTX3-expressing cells. Further work will be required to identify and sort tendon cell subsets. For example, PTX3_PAPPA cells were found to be CD10+CD26+ CD54+ but no clear surface markers were found for DCN_LUM cells based on the very limited set of monoclonal antibodies used in the present study.

The study was limited to cells from one type of tendon, a short period of *in vitro* culture and only two different culture conditions. It is still not clear how to define normal tendon cell behaviour *in vitro* and which culture conditions are optimal. As with many *in vitro* studies of tenocytes, expanding explanted cells to passage 1 before culturing on PDO fibres was necessary. Culturing explanted tenocytes to passage 1 in growth media has additional limitations, including the loss of myofibroblast cell types and induction of gene expression changes including the upregulation of surface markers such as CD90 and other pro-inflammatory factors. Confounding transcriptomic variation remains a significant limitation of single-cell RNA sequencing and further emphasises the importance of validating any transcriptomic descriptive findings.

Results demonstrated that discrete cell clusters could be identified by specific gene and surface protein signatures when human hamstring tendon cells were cultured *in vitro*. The presence of multiple types of human tendon cells and their persistence in culture question the relevance of ongoing investigations that rely on the pooled responses of unsorted tendon cells. It remains to be seen whether there is any functional relevance to the described cell clusters and ongoing *in vitro* interrogation of subset behaviour and phenotypic stability is likely to require consideration of culture surfaces.

Conclusion

Combined single-cell transcriptomics and proteomics of human hamstring tendon cells demonstrated multiple discrete clusters that persisted *in vitro* culture. 4 cell clusters closely resembled *ex vivo* human tendon cell clusters in their gene expression profile: PTX3_PAPPA, ITGA7_NES, DCN_LUM and POSTN_KRT7 cells. Culture on aligned PDO electrospun fibres favoured DCN_LUM, POSTN_SCX and PTX3_PAPPA cells, maintaining expression of common tendon matrix genes and upregulating gene sets enriched for inflammatory signalling. Surface proteomics revealed markers by which 3 of these cell populations could be isolated: PTX3_PAPPA cells were CD10+CD26+CD54+. ITGA7_NES cells were CD146+ and POSTN_SCX cells were CD90+CD95+CD10+. *PTX3*-expressing cells have been implicated in chronic tendon disease. By demonstrating that they are CD10+CD26+CD54+, proliferate on aligned PDO fibres and upregulate gene sets associated with TNF-α and IFN-γ, the study provided an opportunity to interrogate further these disease-associated cells *in vitro*.

This study advanced the understanding of tenocyte subpopulations and informed the design of *in vitro* models of tendon disease. Expanding the repertoire of surface targets in future CITE-Seq studies would benefit the identification and isolation of additional *in vitro* tenocyte populations. Future research should discover additional scaffold materials and culture conditions that preferentially select for reparative tenocyte subpopulations. These advances will help accelerate the development of implants for improved tendon healing and precision therapeutics of chronic tendinopathy.

Acknowledgements

We would like to thank the Oxford Genomics Centre.

There are no competing interests.

This study received ethical approval from the Oxford Musculoskeletal Biobank, a research tissue bank with overarching ethical approval from NHS Research Ethics Committee- South Central- Oxford C (reference 19/SC/0134) to collect, store and release musculoskeletal tissue.

References

Akbar M, MacDonald L, Crowe LAN, Carlberg K, Kurowska-Stolarska M, Ståhl PL, Snelling SJB, McInnes IB, Millar NL (2021) Single cell and spatial transcriptomics in human tendon disease indicate dysregulated immune homeostasis. Ann Rheum Dis **80**: 1494-1497.

Albers IS, Zwerver J, Diercks RL, Dekker JH, Van den Akker-Scheek I (2016) Incidence and prevalence of lower extremity tendinopathy in a Dutch general practice population: a cross sectional study. BMC Musculoskelet Dis **17**: 16. DOI: 10.1186/s12891-016-0885-2.

Bashur CA, Shaffer RD, Dahlgren LA, Guelcher SA, Goldstein AS (2009) Effect of fiber diameter and alignment of electrospun polyurethane meshes on mesenchymal progenitor cells. Tissue Eng Part A **15**: 2435-2445.

Becht E, McInnes L, Healy J, Dutertre C-A, Kwok IWH, Ng LG, Ginhoux F, Newell EW (2019) Dimensionality reduction for visualizing single-cell data using UMAP. Nat Biotechnol **37**: 38-44.

Butler A, Hoffman P, Smibert P, Papalexi E, Satija R (2018) Integrating single-cell transcriptomic data across different conditions, technologies, and species. Nat Biotechnol **36**: 411-420.

Dakin SG, Newton J, Martinez FO, Hedley R, Gwilym S, Jones N, Reid HAB, Wood S, Wells G, Appleton L, Wheway K, Watkins B, Carr AJ (2018) Chronic inflammation is a feature of Achilles tendinopathy and rupture. Br J Sports Med **52**: 359-367.

Dakin SG, Ly L, Colas RA, Oppermann U, Wheway K, Watkins B, Dalli J, Carr AJ (2017)

Increased 15-PGDH expression leads to dysregulated resolution responses in stromal cells from patients with chronic tendinopathy. Sci Rep **7**: 11009. DOI: 10.1038/s41598-017-11188-y.

de Jonge S, van den Berg C, de Vos RJ, van der Heide HJ, Weir A, Verhaar JA, Bierma-Zeinstra SM, Tol JL (2011) Incidence of midportion Achilles tendinopathy in the general population. Br J Sports Med **45**: 1026-1028.

Fleischer S, Miller J, Hurowitz H, Shapira A, Dvir T (2015) Effect of fiber diameter on the assembly of functional 3D cardiac patches. Nanotechnology **26**: 291002. DOI: 10.1088/0957-4484/26/29/291002.

Forouzanfar MH, Alexander L, Anderson HR, Bachman VF, Biryukov S, Brauer M, Burnett R, Casey D, Coates MM, Cohen A, Delwiche K, Estep K, Frostad JJ, Astha KC, Kyu HH, Moradi-Lakeh M, Ng M, Slepak EL, Thomas BA, Wagner J, Aasvang GM, Abbafati C, Abbasoglu Ozgoren A, Abd-Allah F, Abera SF, Aboyans V, Abraham B, Abraham JP, Abubakar I, Abu-Rmeileh NM, Aburto TC, Achoki T, Adelekan A, Adofo K, Adou AK, Adsuar JC, Afshin A, Agardh EE, Al Khabouri MJ, Al Lami FH, Alam SS, Alasfoor D, Albittar MI, Alegretti MA, Aleman AV, Alemu ZA, Alfonso-Cristancho R, Alhabib S, Ali R, Ali MK, Alla F, Allebeck P, Allen PJ, Alsharif U, Alvarez E, Alvis-Guzman N, Amankwaa AA, Amare AT, Ameh EA, Ameli O, Amini H, Ammar W, Anderson BO, Antonio CA, Anwari P, Argeseanu Cunningham S, Arnlöv J, Arsenijevic VS, Artaman A, Asghar RJ, Assadi R, Atkins LS, Atkinson C, Avila MA, Awuah B, Badawi A, Bahit MC, Bakfalouni T, Balakrishnan K, Balalla S, Balu RK, Banerjee A, Barber RM, Barker-Collo SL, Barquera S, Barregard L, Barrero LH, Barrientos-Gutierrez T, Basto-Abreu AC, Basu A, Basu S, Basulaiman MO, Batis Ruvalcaba C, Beardsley J, Bedi N, Bekele T, Bell ML, Benjet C, Bennett DA, Benzian H, Bernabé E, Beyene TJ, Bhala N, Bhalla A, Bhutta ZA, Bikbov B, Bin Abdulhak AA, Blore JD, Blyth FM, Bohensky MA, Bora Başara B, Borges G, Bornstein NM, Bose D, Boufous S, Bourne RR, Brainin M, Brazinova A, Breitborde NJ, Brenner H, Briggs AD, Broday DM, Brooks PM, Bruce NG, Brugha TS, Brunekreef B, Buchbinder R, Bui LN, Bukhman G, Bulloch AG, Burch M, Burney PG, Campos-Nonato IR, Campuzano JC, Cantoral AJ, Caravanos J, Cárdenas R, Cardis E, Carpenter DO, Caso V, Castañeda-Orjuela CA, Castro RE, Catalá-López F, Cavalleri F, Çavlin A, Chadha VK, Chang JC, Charlson FJ, Chen H, Chen W, Chen Z, Chiang PP, Chimed-Ochir O, Chowdhury R, Christophi CA, Chuang TW, Chugh SS, Cirillo M, Claßen TK, Colistro V, Colomar M, Colquhoun SM, Contreras AG, Cooper C, Cooperrider K, Cooper LT, Coresh J, Courville KJ, Criqui MH, Cuevas-Nasu L, Damsere-Derry J, Danawi H, Dandona L, Dandona R, Dargan PI, Davis A, Davitoiu DV, Dayama A, de Castro EF, De la Cruz-Góngora V, De Leo D, de Lima G, Degenhardt L, del Pozo-Cruz B, Dellavalle RP, Deribe K, Derrett S, Des Jarlais DC, Dessalegn M, deVeber GA, Devries KM, Dharmaratne SD, Dherani MK, Dicker D, Ding EL, Dokova K, Dorsey ER, Driscoll TR, Duan L, Durrani AM, Ebel BE, Ellenbogen RG, Elshrek YM, Endres M, Ermakov SP, Erskine HE, Eshrati B, Esteghamati A, Fahimi S, Faraon EJ, Farzadfar F, Fay DF, Feigin VL, Feigl AB, Fereshtehnejad SM, Ferrari AJ, Ferri CP, Flaxman AD, Fleming TD, Foigt N, Foreman KJ, Paleo UF, Franklin RC, Gabbe B, Gaffikin L, Gakidou E, Gamkrelidze A, Gankpé FG, Gansevoort RT, García-Guerra FA, Gasana E, Geleijnse JM, Gessner BD, Gething P, Gibney KB, Gillum RF, Ginawi IA, Giroud M, Giussani G, Goenka S, Goginashvili K, Gomez Dantes H, Gona P, Gonzalez de Cosio T, González-Castell D, Gotay CC, Goto A, Gouda HN, Guerrant RL, Gugnani HC, Guillemin F, Gunnell D, Gupta R, Gupta R, Gutiérrez RA, Hafezi-Nejad N, Hagan H, Hagstromer M, Halasa YA, Hamadeh RR, Hammami M, Hankey GJ, Hao Y, Harb HL, Haregu TN, Haro JM, Havmoeller R, Hay SI, Hedayati MT, Heredia-Pi IB, Hernandez L, Heuton KR, Heydarpour P, Hijar M, Hoek HW, Hoffman HJ, Hornberger JC, Hosgood HD, Hoy DG, Hsairi M, Hu G, Hu H, Huang C, Huang JJ, Hubbell BJ, Huiart L, Husseini A, Iannarone ML, Iburg KM, Idrisov BT, Ikeda N, Innos K, Inoue M, Islami F, Ismayilova S, Jacobsen KH, Jansen HA, Jarvis DL, Jassal SK, Jauregui A, Jayaraman S, Jeemon P, Jensen PN, Jha V, Jiang F, Jiang G, Jiang Y, Jonas JB, Juel K, Kan H, Kany Roseline SS, Karam NE, Karch A, Karema CK, Karthikeyan G, Kaul A, Kawakami N, Kazi DS, Kemp AH, Kengne AP, Keren A, Khader YS, Khalifa SE, Khan EA, Khang YH, Khatibzadeh S, Khonelidze I, Kieling C, Kim D, Kim S, Kim Y, Kimokoti RW, Kinfu Y, Kinge JM, Kissela BM, Kivipelto M, Knibbs LD, Knudsen AK, Kokubo Y, Kose MR, Kosen S, Kraemer A, Kravchenko M, Krishnaswami S, Kromhout H, Ku T, Kuate Defo B, Kucuk Bicer B, Kuipers EJ, Kulkarni C, Kulkarni VS, Kumar GA, Kwan GF, Lai T, Lakshmana Balaji A, Lalloo R, Lallukka T, Lam H, Lan Q, Lansingh VC, Larson HJ, Larsson A, Laryea DO, Lavados PM, Lawrynowicz AE, Leasher JL, Lee JT, Leigh J, Leung R, Levi M, Li Y, Li Y, Liang J, Liang X, Lim SS, Lindsay MP, Lipshultz SE, Liu S, Liu Y, Lloyd BK, Logroscino G, London SJ, Lopez N, Lortet-Tieulent J, Lotufo PA, Lozano R, Lunevicius R, Ma J, Ma S, Machado VM, MacIntyre MF, Magis-Rodriguez C, Mahdi AA, Majdan M, Malekzadeh R, Mangalam S, Mapoma CC, Marape M, Marcenes W, Margolis DJ, Margono C, Marks GB, Martin RV, Marzan MB, Mashal MT, Masiye F, Mason-Jones AJ, Matsushita K, Matzopoulos R, Mayosi BM, Mazorodze TT, McKay AC, McKee M, McLain A, Meaney PA, Medina C, Mehndiratta MM, Mejia-Rodriguez F, Mekonnen W, Melaku YA, Meltzer M, Memish ZA, Mendoza W, Mensah GA, Meretoja A, Mhimbira FA, Micha R, Miller TR, Mills EJ, Misganaw A, Mishra S, Mohamed Ibrahim N, Mohammad KA, Mokdad AH, Mola GL, Monasta L, Montañez Hernandez JC, Montico M, Moore AR, Morawska L, Mori R, Moschandreas J, Moturi WN, Mozaffarian D, Mueller UO, Mukaigawara M, Mullany EC, Murthy KS, Naghavi M, Nahas Z, Naheed A, Naidoo KS, Naldi L, Nand D, Nangia V,

Narayan KM, Nash D, Neal B, Nejjari C, Neupane SP, Newton CR, Ngalesoni FN, Ngirabega Jde D, Nguyen G, Nguyen NT, Nieuwenhuijsen MJ, Nisar MI, Nogueira JR, Nolla JM, Nolte S, Norheim OF, Norman RE, Norrving B, Nyakarahuka L, Oh IH, Ohkubo T, Olusanya BO, Omer SB, Opio JN, Orozco R, Pagcatipunan RS, Jr., Pain AW, Pandian JD, Panelo CI, Papachristou C, Park EK, Parry CD, Paternina Caicedo AJ, Patten SB, Paul VK, Pavlin BI, Pearce N, Pedraza LS, Pedroza A, Pejin Stokic L, Pekericli A, Pereira DM, Perez-Padilla R, Perez-Ruiz F, Perico N, Perry SA, Pervaiz A, Pesudovs K, Peterson CB, Petzold M, Phillips MR, Phua HP, Plass D, Poenaru D, Polanczyk GV, Polinder S, Pond CD, Pope CA, Pope D, Popova S, Pourmalek F, Powles J, Prabhakaran D, Prasad NM, Qato DM, Quezada AD, Quistberg DA, Racapé L, Rafay A, Rahimi K, Rahimi-Movaghar V, Rahman SU, Raju M, Rakovac I, Rana SM, Rao M, Razavi H, Reddy KS, Refaat AH, Rehm J, Remuzzi G, Ribeiro AL, Riccio PM, Richardson L, Riederer A, Robinson M, Roca A, Rodriguez A, Rojas-Rueda D, Romieu I, Ronfani L, Room R, Roy N, Ruhago GM, Rushton L, Sabin N, Sacco RL, Saha S, Sahathevan R, Sahraian MA, Salomon JA, Salvo D, Sampson UK, Sanabria JR, Sanchez LM, Sánchez-Pimienta TG, Sanchez-Riera L, Sandar L, Santos IS, Sapkota A, Satpathy M, Saunders JE, Sawhney M, Saylan MI, Scarborough P, Schmidt JC, Schneider IJ, Schöttker B, Schwebel DC, Scott JG, Seedat S, Sepanlou SG, Serdar B, Servan-Mori EE, Shaddick G, Shahraz S, Levy TS, Shangguan S, She J, Sheikhbahaei S, Shibuya K, Shin HH, Shinohara Y, Shiri R, Shishani K, Shiue I, Sigfusdottir ID, Silberberg DH, Simard EP, Sindi S, Singh A, Singh GM, Singh JA, Skirbekk V, Sliwa K, Soljak M, Soneji S, Søreide K, Soshnikov S, Sposato LA, Sreeramareddy CT, Stapelberg NJ, Stathopoulou V, Steckling N, Stein DJ, Stein MB, Stephens N, Stöckl H, Straif K, Stroumpoulis K, Sturua L, Sunguya BF, Swaminathan S, Swaroop M, Sykes BL, Tabb KM, Takahashi K, Talongwa RT, Tandon N, Tanne D, Tanner M, Tavakkoli M, Te Ao BJ, Teixeira CM, Téllez Rojo MM, Terkawi AS, Texcalac-Sangrador JL, Thackway SV, Thomson B, Thorne-Lyman AL, Thrift AG, Thurston GD, Tillmann T, Tobollik M, Tonelli M, Topouzis F, Towbin JA, Toyoshima H, Traebert J, Tran BX, Trasande L, Trillini M, Trujillo U, Dimbuene ZT, Tsilimbaris M, Tuzcu EM, Uchendu US, Ukwaja KN, Uzun SB, van de Vijver S, Van Dingenen R, van Gool CH, van Os J, Varakin YY, Vasankari TJ, Vasconcelos AM, Vavilala MS, Veerman LJ, Velasquez-Melendez G, Venketasubramanian N, Vijayakumar L, Villalpando S, Violante FS, Vlassov VV, Vollset SE, Wagner GR, Waller SG, Wallin MT, Wan X, Wang H, Wang J, Wang L, Wang W, Wang Y, Warouw TS, Watts CH, Weichenthal S, Weiderpass E, Weintraub RG, Werdecker A, Wessells KR, Westerman R, Whiteford HA, Wilkinson JD, Williams HC, Williams TN, Woldeyohannes SM, Wolfe CD, Wong JQ, Woolf AD, Wright JL, Wurtz B, Xu G, Yan LL, Yang G, Yano Y, Ye P, Yenesew M, Yentür GK, Yip P, Yonemoto N, Yoon SJ, Younis MZ, Younoussi Z, Yu C, Zaki ME, Zhao Y, Zheng Y, Zhou M, Zhu J, Zhu S, Zou X, Zunt JR, Lopez AD, Vos T, Murray CJ (2015) Global, regional, and national comparative risk assessment of 79 behavioural, environmental and occupational, and metabolic risks or clusters of risks in 188 countries, 1990-2013: a systematic analysis for the Global Burden of Disease Study 2013. Lancet **386**: 2287-2323.

Garcia-Melchor E, Cafaro G, MacDonald L, Crowe LAN, Sood S, McLean M, Fazzi UG, McInnes IB, Akbar M, Millar NL (2021) Novel self-amplificatory loop between T cells and tenocytes as a driver of chronicity in tendon disease. Ann Rheum Dis **80**: 1075-1085.

Giordani L, He GJ, Negroni E, Sakai H, Law JYC, Siu MM, Wan R, Corneau A, Tajbakhsh S, Cheung TH, Le Grand F (2019) High-dimensional single-cell cartography reveals novel skeletal muscle-resident cell populations. Molecular Cell **74**: 609-621.

Gomes SR, Rodrigues G, Martins GG, Roberto MA, Mafra M, Henriques CM, Silva JC (2015) *In vitro* and *in vivo* evaluation of electrospun nanofibers of PCL, chitosan and gelatin: a comparative study. Mater Sci Eng C Mater Biol Appl **46**: 348-358.

Hakimi O, Mouthuy PA, Zargar N, Lostis E, Morrey M, Carr A (2015) A layered electrospun and woven surgical scaffold to enhance endogenous tendon repair. Acta Biomater **26**: 124-135.

Hakimi O, Ternette N, Murphy R, Kessler BM, Carr A (2017) A quantitative label-free analysis of the extracellular proteome of human supraspinatus tendon reveals damage to the pericellular and elastic fibre niches in torn and aged tissue. PLoS One **12**: e0177656. DOI: 10.1371/journal.pone.0177656.

Harvey T, Flamenco S, Fan C-M (2019) A Tppp3+Pdgfra+ tendon stem cell population contributes to regeneration and reveals a shared role for PDGF signalling in regeneration and fibrosis. Nature Cell Biology **21**: 1490-1503.

Kendal A, Snelling S, Dakin S, Stace E, Mouthuy PA, Carr A (2017) Resorbable electrospun polydioxanone fibres modify the behaviour of cells from both healthy and diseased human tendons. Eur Cell Mater **33**: 169-182.

Kendal AR, Layton T, Al-Mossawi H, Appleton L, Dakin S, Brown R, Loizou C, Rogers M, Sharp R, Carr A (2020) Multi-omic single cell analysis resolves novel stromal cell populations in healthy and diseased human tendon. Sci Rep **10**: 13939. DOI: 10.1038/s41598-020-70786-5.

Kim DH, Han K, Gupta K, Kwon KW, Suh KY, Levchenko A (2009) Mechanosensitivity of fibroblast cell shape and movement to anisotropic substratum topography gradients. Biomaterials **30**: 5433-5444.

Lee CH, Shin HJ, Cho IH, Kang YM, Kim IA, Park KD, Shin JW (2005) Nanofiber alignment and direction of mechanical strain affect the ECM production of human ACL fibroblast. Biomaterials **26**: 1261-1270.

Martins JA, Lach AA, Morris HL, Carr AJ, Mouthuy PA (2020) Polydioxanone implants: A systematic review on safety and performance in patients. J Biomater Appl **34**: 902-916.

Mouthuy PA, Zargar N, Hakimi O, Lostis E, Carr A (2015) Fabrication of continuous electrospun filaments with potential for use as medical fibres. Biofabrication **7**: 025006. DOI: 10.1088/1758-5090/7/2/025006.

Nezhentsev A, Abhari R, Baldwin MJ, Mimpen J, Augustyniak E, Isaacs M, Mouthuy PA, Carr AJ, Snelling S (2021) *In vitro* evaluation of the response of human tendon-derived stromal cells to a novel electrospun suture for tendon repair. Transl Sports Med **4**: 409-418.

Riel H, Lindstrøm CF, Rathleff MS, Jensen MB, Olesen JL (2019) Prevalence and incidence rate of lower-extremity tendinopathies in a Danish general practice: a registry-based study. BMC Musculoskelet Disord **20**: 239. DOI: 10.1186/s12891-019-2629-6.

Schaum N, Karkanias J, Neff NF, May AP, Quake SR, Wyss-Coray T, Darmanis S, Batson J, Botvinnik O, Chen MB, Chen S, Green F, Jones RC, Maynard A, Penland L, Pisco AO, Sit RV, Stanley GM, Webber JT, Zanini F, Baghel AS, Bakerman I, Bansal I, Berdnik D, Bilen B, Brownfield D, Cain C, Chen MB, Chen S, Cho M, Cirolia G, Conley SD, Darmanis S, Demers A, Demir K, de Morree A, Divita T, du Bois H, Dulgeroff LBT, Ebadi H, Espinoza FH, Fish M, Gan Q, George BM, Gillich A, Green F, Genetiano G, Gu X, Gulati GS, Hang Y, Hosseinzadeh S, Huang A, Iram T, Isobe T, Ives F, Jones RC, Kao KS, Karnam G, Kershner AM, Kiss BM, Kong W, Kumar ME, Lam JY, Lee DP, Lee SE, Li G, Li Q, Liu L, Lo A, Lu W-J, Manjunath A, May AP, May KL, May OL, Maynard A, McKay M, Metzger RJ, Mignardi M, Min D, Nabhan AN, Neff NF, Ng KM, Noh J, Patkar R, Peng WC, Penland L, Puccinelli R, Rulifson EJ, Schaum N, Sikandar SS, Sinha R, Sit RV, Szade K, Tan W, Tato C, Tellez K, Travaglini KJ, Tropini C, Waldburger L, van Weele LJ, Wosczyna MN, Xiang J, Xue S, Youngyunpipatkul J, Zanini F, Zardeneta ME, Zhang F, Zhou L, Bansal I, Chen S, Cho M, Cirolia G, Darmanis S, Demers A, Divita T, Ebadi H, Genetiano G, Green F, Hosseinzadeh S, Ives F, Lo A, May AP, Maynard A, McKay M, Neff NF, Penland L, Sit RV, Tan W, Waldburger L, Youngyunpipatkul J, Batson J, Botvinnik O, Castro P, Croote D, Darmanis S, DeRisi JL, Karkanias J, Pisco AO, Stanley GM, Webber JT, Zanini F, Baghel AS, Bakerman I, Batson J, Bilen B, Botvinnik O, Brownfield D, Chen MB, Darmanis S, Demir K, de Morree A, Ebadi H, Espinoza FH, Fish M, Gan Q, George BM, Gillich A, Gu X, Gulati GS, Hang Y, Huang A, Iram T, Isobe T, Karnam G, Kershner AM, Kiss BM, Kong W, Kuo CS, Lam JY, Lehallier B, Li G, Li Q, Liu L, Lu W-J, Min D, Nabhan AN, Ng KM, Nguyen PK, Patkar R, Peng WC, Penland L, Rulifson EJ, Schaum N, Sikandar SS, Sinha R, Szade K, Tan SY, Tellez K, Travaglini KJ, Tropini C, van Weele LJ, Wang BM, Wosczyna MN, Xiang J, Yousef H, Zhou L, Batson J, Botvinnik O, Chen S, Darmanis S, Green F, May AP, Maynard A, Pisco AO, Quake SR, Schaum N, Stanley GM, Webber JT, Wyss-Coray T, Zanini F, Beachy PA, Chan CKF, de Morree A, George BM, Gulati GS, Hang Y, Huang KC, Iram T, Isobe T, Kershner AM, Kiss BM, Kong W, Li G, Li Q, Liu L, Lu W-J, Nabhan AN, Ng KM, Nguyen PK, Peng WC, Rulifson EJ, Schaum N, Sikandar SS, Sinha R, Szade K, Travaglini KJ, Tropini C, Wang BM, Weinberg K, Wosczyna MN, Wu SM, Yousef H, Barres BA, Beachy PA, Chan CKF, Clarke MF, Darmanis S, Huang KC, Karkanias J, Kim SK, Krasnow MA, Kumar ME, Kuo CS, May AP, Metzger RJ, Neff NF, Nusse R, Nguyen PK, Rando TA, Sonnenburg J, Wang BM, Weinberg K, Weissman IL, Wu SM, Quake SR, Wyss-Coray T, The Tabula Muris C, Overall c, Logistical c, Organ c, processing, Library p, sequencing, Computational data a, Cell type a, Writing g, Supplemental text writing g, Principal i (2018) Single-cell transcriptomics of 20 mouse organs creates a Tabula Muris. Nature **562**: 367-372.

Smith RD, Carr A, Dakin SG, Snelling SJ, Yapp C, Hakimi O (2016) The response of tenocytes to commercial scaffolds used for rotator cuff repair. Eur Cell Mater **31**: 107-118.

Still C, Chang W-T, Sherman SL, Sochacki KR, Dragoo JL, Qi LS (2021) Single-cell transcriptomic profiling reveals distinct mechanical responses between normal and diseased tendon progenitor cells. Cell Rep Med **2**: 100343.

Stolk M, Klatte-Schulz F, Schmock A, Minkwitz S, Wildemann B, Seifert M (2017) New insights into tenocyte-immune cell interplay in an *in vitro* model of inflammation. Sci Rep **7**: 9801. DOI: 10.1038/s41598-017-09875-x.

Yin Z, Hu JJ, Yang L, Zheng ZF, An CR, Wu BB, Zhang C, Shen WL, Liu HH, Chen JL, Heng BC, Guo GJ, Chen X, Ouyang HW (2016) Single-cell analysis reveals a nestin(+) tendon stem/progenitor cell population with strong tenogenic potentiality. Sci Adv **2**: e1600874. DOI: 10.1126/sciadv.1600874.

Web References

1. https://citeseq.files.wordpress.com/2019/02/cite-seq_and_hashing_protocol_190213.pdf [17-05-2022]

2. https://citeseq.files.wordpress.com/2019/02/cite-seq_and_hashing_protocol_190213.pdf [17-05-2022]

3. satijalab.org/seurat [17-05-2022]

Discussion with Reviewers

Reviewer 1: What effect do you think the loss of endothelial, immune and other tendon cell populations will have on the fibroblast-like populations you have studied? Is the loss of crosstalk with these populations likely to have an effect on their transcriptome and behaviour?

Authors: The loss of endothelial cell populations in vitro is likely to interrupt NOTCH3-mediated signalling in CD90+ fibroblasts. NOTCH3 signalling

emanating from vascular endothelial cells helps drive differentiation of fibroblasts into mural fibroblasts and a drastic reduction in this population was observed *in vitro.* It is also likely that the loss of pro-resolution macrophages *in vitro* leads to increased stress of stromal populations, possibly contributing to the upregulation of CD90+ and other activated fibroblast markers.

Reviewer 2: How comparable were the tendon cell populations that were analysed after expansion in *in vitro* culture to tendon cell populations in native tissue?
Authors: 4 *in vitro* populations closely matched the native tissue populations (PTX3_PAPPA matched native tissue tenocyte A, POSTN_SCX matched native tissue tenocyte B, ITGA7_NES matched native tissue tenocyte C and DNC_LUM matched native tissue tenocyte D). While the general transcriptomic signatures matched 4 of the native populations, an upregulation of fibroblast activation markers, including *THY1*, *STAT6* and *FAP*, was observed in the *in vitro* clusters. One native tissue fibroblast subtype cell type that was notably missing in the *in vitro* analysis was the tenocyte E TPPP + THY1 – a tenocyte population that resides in the tendon sheath and has been proposed as a tendon stem cell. Probably, this population gets outcompeted *in vitro* by more fibrotic/collagen-depositing CD90+ cell subtypes. It will be important to conduct further experiments to identify appropriate methods and scaffolds to study this tenocyte population, as it might play a role in repairing tendon damage.

Reviewer 2: Can you critically discuss differences between *in vivo* healing, where cells migrate to the wound site, synthesising and remodelling their own extracellular matrix over time, and an approach where cells are seeded onto a scaffold that already mimics a mature tendon matrix?
Authors: *In vivo* natural tendon healing involves the sequential but partially overlapping stages of 1) inflammation, 2) proliferation, 3) matrix remodelling. Inflammation involves the migration of cells from the tendon sheath and interfasicular matrix (putative TPPP+ TPSC populations) into matrix-dense damaged regions. This process involves crosstalk between endothelial, immune and stromal populations across a gradient of different cell states, involving several bioactive molecules including TGF-B, FGFs, PDGFs, VEGF, CTGF and MMPs. The proliferation of stromal cells leads to the deposition of collagen 3 to repair damaged tendon matrix, which can then be remodelled and replaced by the stronger and better aligned collagen 1 in a process that may continue for months or years. A disadvantage of naturally healing tendon is that a repaired tendon has higher rates of injury than a normal healthy tendon and, especially in older populations, the healing process can become characterised by chronic inflammation and pain. Biological and synthetic scaffolds seeded with tendon cells offer the promise of a faster and enhanced tendon healing by providing damaged tendon with the mechanical environment, strength and cues necessary for tenocytes to repair damaged tendon. However, when culturing cells *in vitro* and seeding onto scaffolds, we are pre-selecting populations that preferentially survive on specific scaffolds and losing tenocyte populations that might be critical for successful tendon repair. Scaffolds with cells will require careful characterisation of the tenocyte populations that are seeded onto the structure to optimise tendon healing. Fibroblasts grown *in vitro* are known to upregulate CD90, FAP, STAT6 and other known markers of fibroblast activation that could lead to inflammation *in vivo*. Similarly, CD90− cells, such as TPPP+ tendon progenitor stem cells, are missing from these cultures and their absence could impair tendon healing when using implanted scaffolds. Further analysis of tenocyte subsets grown on different scaffold conditions will be necessary to design scaffold-cell constructs that recapitulate natural tendon healing while also providing improved mechanical strength and flexibility to minimise future re-injuries.

Editor's note: The Scientific Editor responsible for this paper was Denitsa Docheva.